Multi-Component (MC) SIMP models with $U(1)_X \to Z_2 \times Z_3$

Pyungwon Ko (KIAS)

CORFU2021
Aug 29 — Sep 9 (2021)

Introduction

WIMP vs. SIMP

- DM # Changes involves the SM sector : e.g. $\chi\chi \to f\bar{f}$

- $\Omega_\chi \sim \frac{6\times 10^{-27} cm^3/s}{<\sigma_{ann} v>} \sim 0.23$ for $<\sigma_{ann} v> \sim 3\times 10^{-26} cm^3/s$

- $<\sigma_{ann} v> \sim \frac{\alpha_w^2}{M^2}$

- For $\alpha_w \sim 0.1$ and $M \sim 1 TeV$, we get $\Omega_X \sim O(0.1)$

- DM # changes occur within the dark sector : e.g. $\chi\chi\chi(\chi) \to \chi\chi$

- For WIMP scenarios, $m_{DM} \sim \alpha_{ann}(T_{eq} M_{Pl})^{1/2}$

- For $3 \to 2$ processes, $m_{DM} \sim \alpha_{eff}(T_{eq}^2 M_{Pl})^{1/3} \sim O(100) MeV$

- For $4 \to 2$ processes, $m_{DM} \sim \alpha_{eff}(T_{eq}^3 M_{Pl})^{1/3} \sim O(100) keV$

[Hochberg et al., 1402.5143]

- sub-GeV DM is well motivated in the SIMP scenarios

Dark QCD + WZW

- Dark flavor symmetry G=SU(N_f)$_L$ x SU(N_f)$_R$ is SSB into diagonal H=SU(N_f)$_V$ by dark QCD condensation
- Effective Lagrangian for NG bosons (dark pions) contain 5-point vertex : WZW term for $\Pi_5(G/H) = Z \ (N_f > 2)$

$$\boxed{\Gamma_{\mathrm{WZ}} = C \int_{M^5} d^5x \ \mathrm{Tr}(\alpha^5) \qquad \text{with} \quad \alpha = dUU^\dagger.}$$

$$\boxed{U = e^{2i\pi/F}} \qquad \boxed{C = -i\frac{N_c}{240\pi^2}}$$

in the absence of external gauge fields

SIMP Dark Mesons

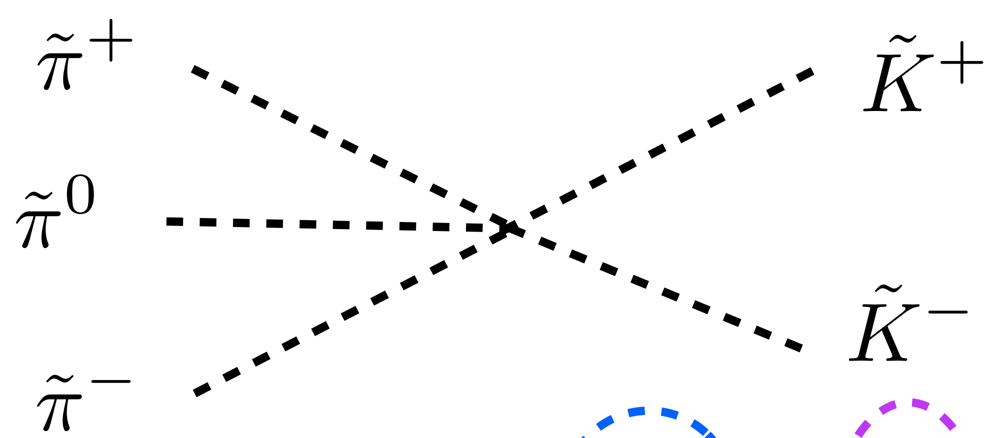

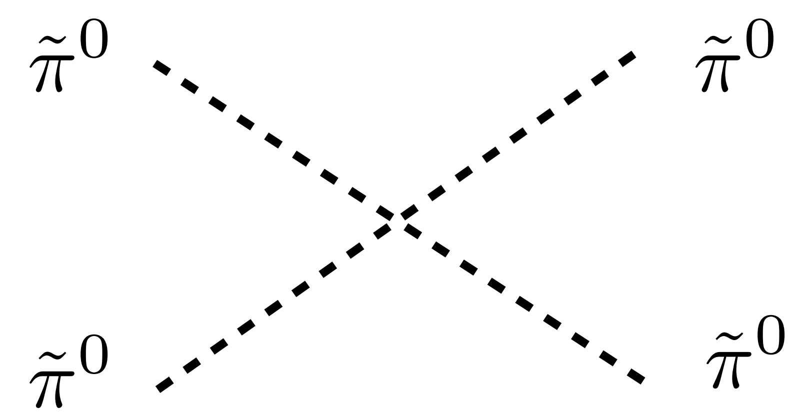

~const ~const

$$\langle \sigma v^2 \rangle_{3\to 2} = \frac{5\sqrt{5} N_c^2 m_\pi^5}{2\pi^5 F^{10}} \frac{t^2}{N_\pi^3} \left(\frac{T_F}{m_\pi} \right)^2, \qquad \sigma_{\text{self}} = \frac{m_\pi^2}{32\pi F^4} \frac{a^2}{N_\pi^2}$$

G_c	G_f/H	N_π	t^2	$N_f^2 a^2$
$SU(N_c)$	$\frac{SU(N_f)\times SU(N_f)}{SU(N_f)}$ $(N_f \geq 3)$	$N_f^2 - 1$	$\frac{4}{3} N_f (N_f^2-1)(N_f^2-4)$	$8(N_f-1)(N_f+1)(3N_f^4 - 2N_f^2 + 6)$
$SO(N_c)$	$SU(N_f)/SO(N_f)$ $(N_f \geq 3)$	$\frac{1}{2}(N_f+2)(N_f-1)$	$\frac{1}{12} N_f (N_f^2-1)(N_f^2-4)$	$(N_f-1)(N_f+2)(3N_f^4+7N_f^3-2N_f^2-12N_f+24)$
$Sp(N_c)$	$SU(2N_f)/Sp(2N_f)$ $(N_f \geq 2)$	$(2N_f+1)(N_f-1)$	$\frac{2}{3} N_f (N_f^2-1)(4N_f^2-1)$	$4(N_f-1)(2N_f+1)(6N_f^4-7N_f^3-N_f^2+3N_f+3)$

[Hochberg, Kuflik, Murayama, Volansky, Wacker, 1411.3727, PRL (2015)]

SIMP Parameter Space

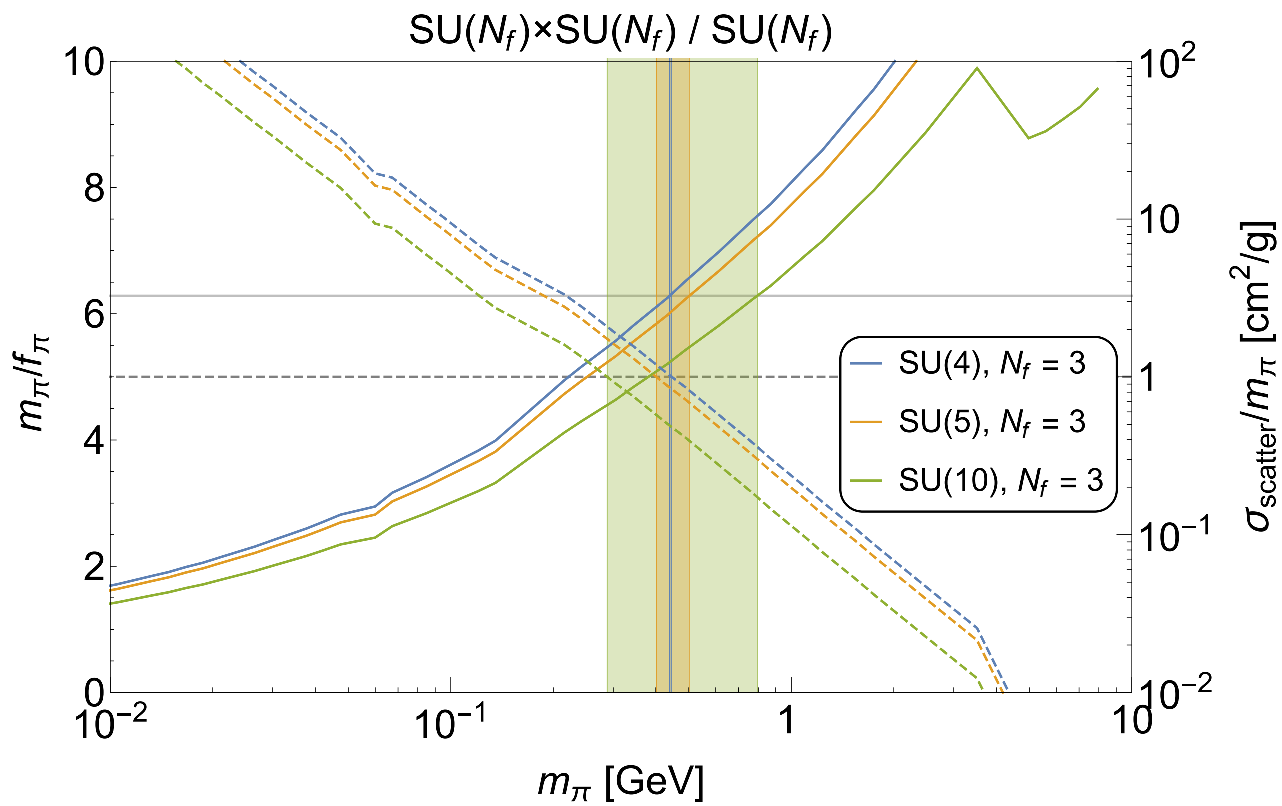

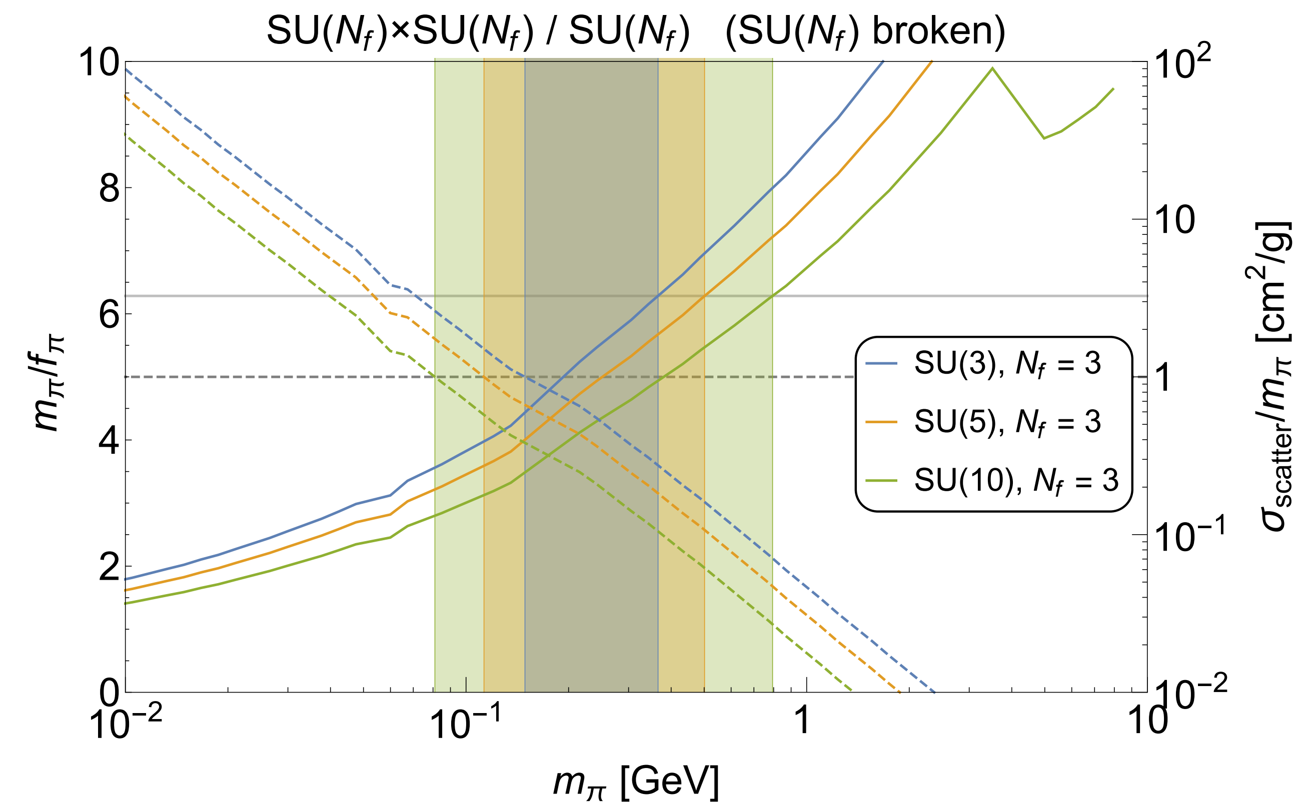

- DM self scattering : $\sigma_{\rm self}/m_{\rm DM} < 1\,{\rm cm}^2/{\rm g}$

Large Nc > 3

- Validity of ChPT : $m_\pi/f_\pi < 2\pi$

More serious in NNLO ChPT
Sannino et al, 1507.01590

SIMP + VDM

With Soo Min Choi, Hyun Min Lee, Alexander Natale,
arXiv:1801.07726, PRD (2018)

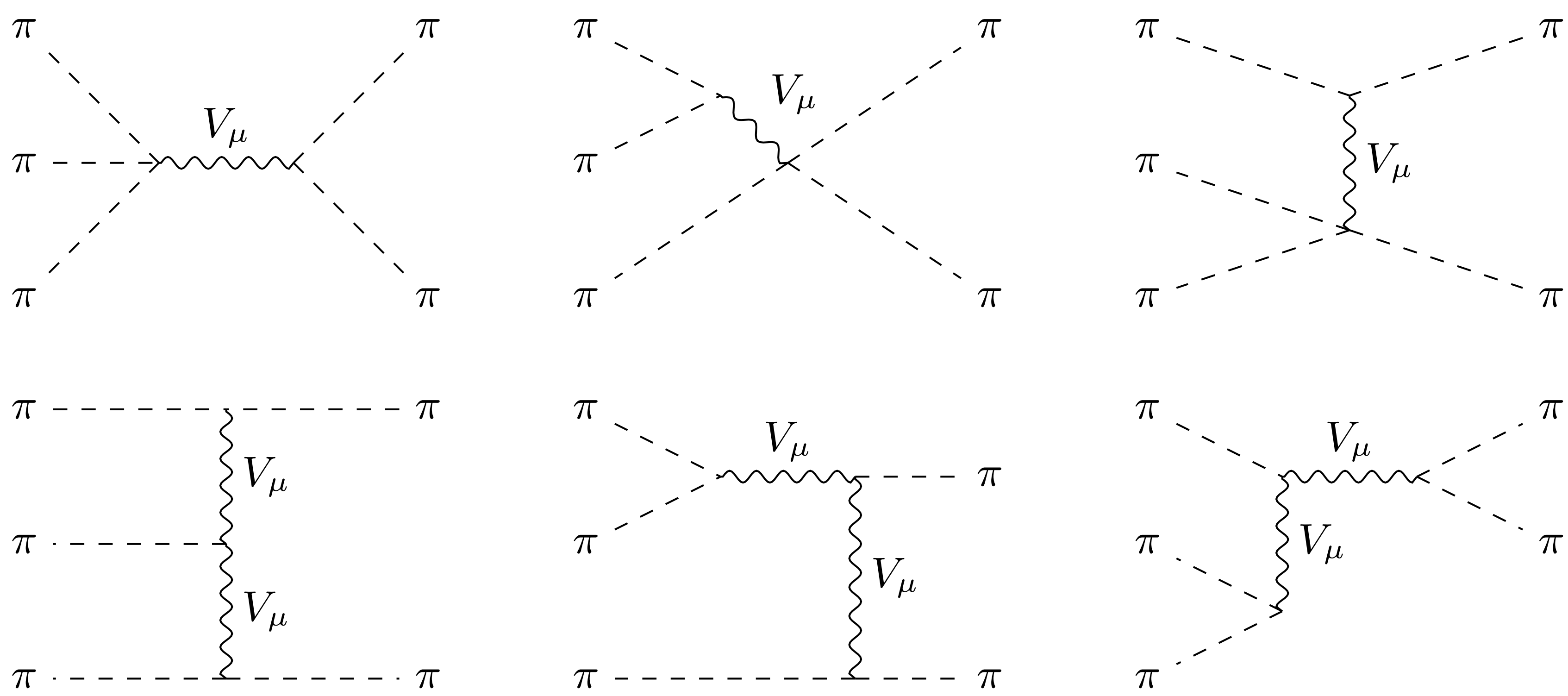

FIG. 1: Feynman diagrams contributing to $3 \to 2$ processes for the dark pions with the vector meson interactions.

SIMP + VM

New diagrams involving dark vector mesons

$$\pi^+\pi^-\pi^0 \to \omega \to K^+K^-(K^0\overline{K^0})$$

$$\gamma = \frac{m_V \Gamma}{9m_\pi^2}, \text{ and } \epsilon = \frac{m_V^2 - 9m_\pi^2}{9m_\pi^2}$$ **(for 3 pi resonance case)**

We choose a small epsilon [say, 0.1 (near resonance)]
and a small gamma (NWA)

Results

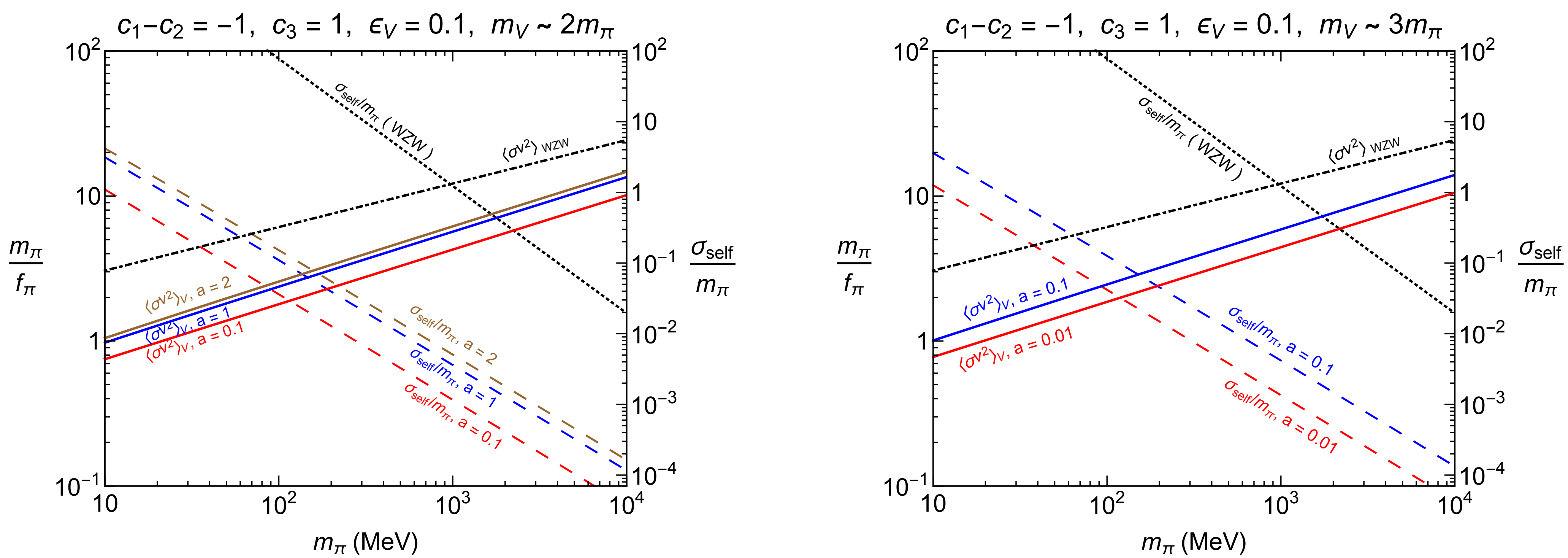

FIG. 2: Contours of relic density ($\Omega h^2 \approx 0.119$) for m_π and m_π/f_π and self-scattering cross section per DM mass in cm^2/g as a function of m_π. The case without and with vector mesons are shown in black lines and colored lines respectively. We have imposed the relic density condition for obtaining the contours of self-scattering cross section. Vector meson masses are taken near the resonances with $m_V = 2(3)m_\pi\sqrt{1+\epsilon_V}$ on left(right) plots. In both plots, $c_1 - c_2 = -1$ and $\epsilon_V = 0.1$ are taken.

- The allowed parameter space is in a better shape now, especially for 2 pi resonance case

Summary for DQCD SIMP

- Hidden (dark) QCD models make an interesting possibility to study the origin of EWSB, (C)DM

- WIMP scenario is still viable, and will be tested to some extent by precise measurements of the Higgs signal strength and by discovery of the singlet scalar, which is however a formidable task unless we are very lucky

- SIMP scenario using 3->2 scattering via WZW term is interesting, but there are a few issues which ask for further study (dark resonance could play an important role for thermal relic and kinetic contact with the SM sector)

Motivations for MC SIMP

- The present Universe made of a single component DM may be too simplified a picture $\longrightarrow$ Multi component DM models interesting and important possibilities

- In case of SIMP models, dark QCD scenario provides multi component SIMP, but it is not really multi component, since they are related with flavor symmetry

- In particular they have the same spins, and the mass difference can not be large : $m_{\rm DM}^2 \sim m_q \Lambda_{\rm conf}$, $\delta m^2 < \Lambda_{\rm confine}^2$

- Let us try to construct multi component SIMP models with different spins and larger mass differences

Motivations (Cont'd)

- In this talk, I present a DM model based on $U(1)_X \to Z_2 \times Z_3$

- Before the main topics, let me discuss DM models based on $U(1)_X \to Z_3$ and $U(1)_X \to Z_2$, respectively, emphasizing the difference between the global and local dark symmetries

- Somewhat long digression on local Z_3 scalar DM model, and local Z_2 scalar and spin-1/2 DM models

Contents

- Introduction
- Scalar DM with $U(1)_X \to Z_3$
- Inelastic DM models with $U(1)_X \to Z_2$ and XENON1T excess
- Multi components SIMP models with $U(1)_X \to Z_2 \times Z_3$
- Comparison with a simple minded EFT approach
- Summary

Scalar DM model with

$$U(1)_X \to Z_3$$

Based on
- P. Ko, Y. Tang, 1402.6449, 1407.5492
- J. Guo, Z. Kang, P. Ko, Y. Orikasa : 1502.00508
- P. Ko, Y. Tang, 2006.15822

Scalar DM with local Z_3 sym

- Consider U(1)x dark gauge symmetry, with scalar DM X and dark Higgs ϕ_X with charges 1 and 3, respectively

$$\mathcal{L} = \mathcal{L}_{\rm SM} - \frac{1}{4}\tilde{X}_{\mu\nu}\tilde{X}^{\mu\nu} - \frac{1}{2}\sin\epsilon\,\tilde{X}_{\mu\nu}\tilde{B}^{\mu\nu} + D_\mu\phi_X^\dagger D^\mu\phi_X + D_\mu X^\dagger D^\mu X - V$$

$$V = -\mu_H^2 H^\dagger H + \lambda_H\left(H^\dagger H\right)^2 - \mu_\phi^2\phi_X^\dagger\phi_X + \lambda_\phi\left(\phi_X^\dagger\phi_X\right)^2 + \mu_X^2 X^\dagger X + \lambda_X\left(X^\dagger X\right)^2$$
$$+ \lambda_{\phi H}\phi_X^\dagger\phi_X H^\dagger H + \lambda_{\phi X}X^\dagger X\phi_X^\dagger\phi_X + \lambda_{HX}X^\dagger X H^\dagger H + \left(\lambda_3 X^3\phi_X^\dagger + H.c.\right)$$

V_X

Global Z3 model by Belanger et al
without ϕ_X and Z'
arXiv:1211.1014 (JCAP)

Comparison with Global Z3 DM

Belanger et al,1211.1014 (JCAP)

$$V_{\rm eff} \simeq -\mu_H^2 H^\dagger H + \lambda_H \left(H^\dagger H\right)^2 + \mu_X^2 X^\dagger X + \lambda_X \left(X^\dagger X\right)^2 + \lambda_{HX} X^\dagger X H^\dagger H + \mu_3 X^3$$
$$+ \text{higher order terms} + H.c,$$

- However global symmetry can be broken by gravity induced nonrenormalizable op's:

$$\frac{1}{\Lambda} X F_{\mu\nu} F^{\mu\nu}$$

Global Z3 "X" with EW scale mass will decay immediately and can not be a DM

- Also particle contents different : Z' and H2
- DM & H phenomenology change a lot

Global vs. Local Z_3 DM

Global Z3
(Belanger, Pukhov et al)

- SM + X
- DD & thermal relic >> $m_X > 120$ GeV
- Vacuum stability >> DD cross section within XENON1T experiment
- No light mediators

Local Z3
(Ko, Yong Tang)

- SM + X, ϕ, Z'
- Additional annihilation channels open
- DD constraints relaxed
- Light m_X allowed
- Light mediator ϕ : strong self interactions of X's

Semi-annihilation

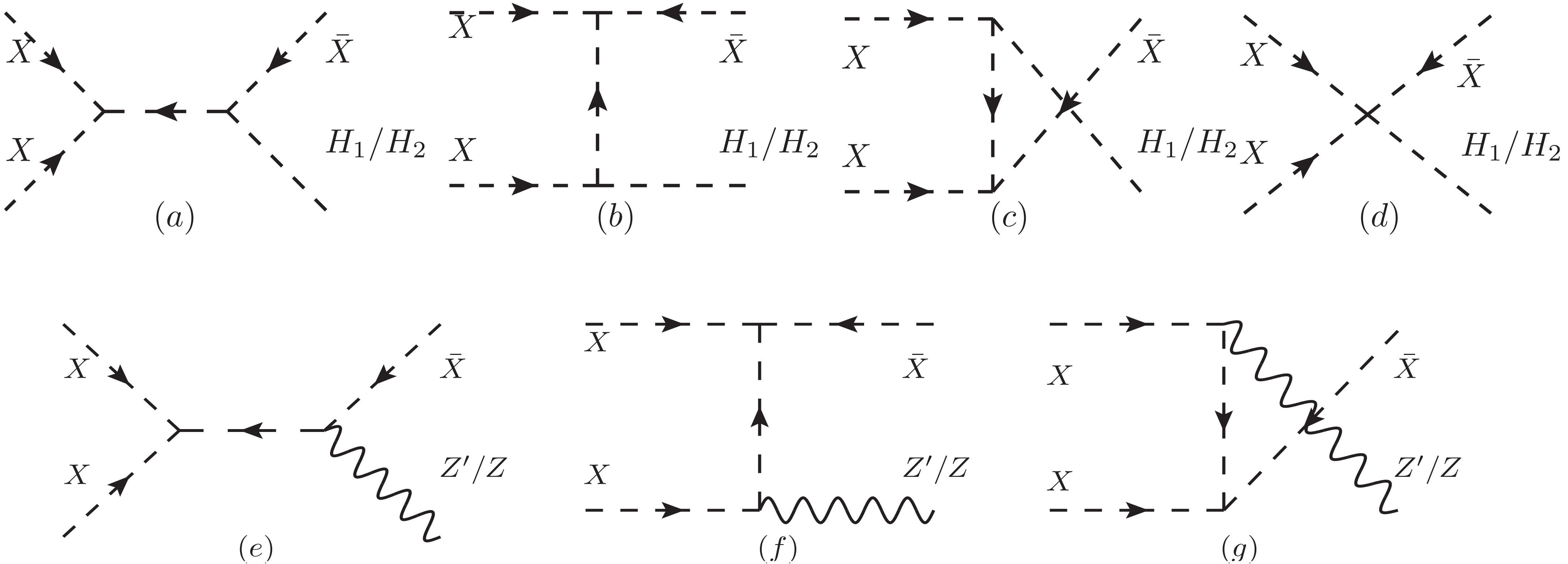

$$\frac{dn_X}{dt} = -v\sigma^{XX^* \to YY}\left(n_X^2 - n_{X\,\mathrm{eq}}^2\right) - \frac{1}{2}v\sigma^{XX\to X^*Y}\left(n_X^2 - n_X n_{X\,\mathrm{eq}}\right) - 3Hn_X,$$

$$r \equiv \frac{1}{2}\frac{v\sigma^{XX\to X^*Y}}{v\sigma^{XX^*\to YY} + \frac{1}{2}v\sigma^{XX\to X^*Y}}.$$

micrOMEGAs

Relic density and Direct Search

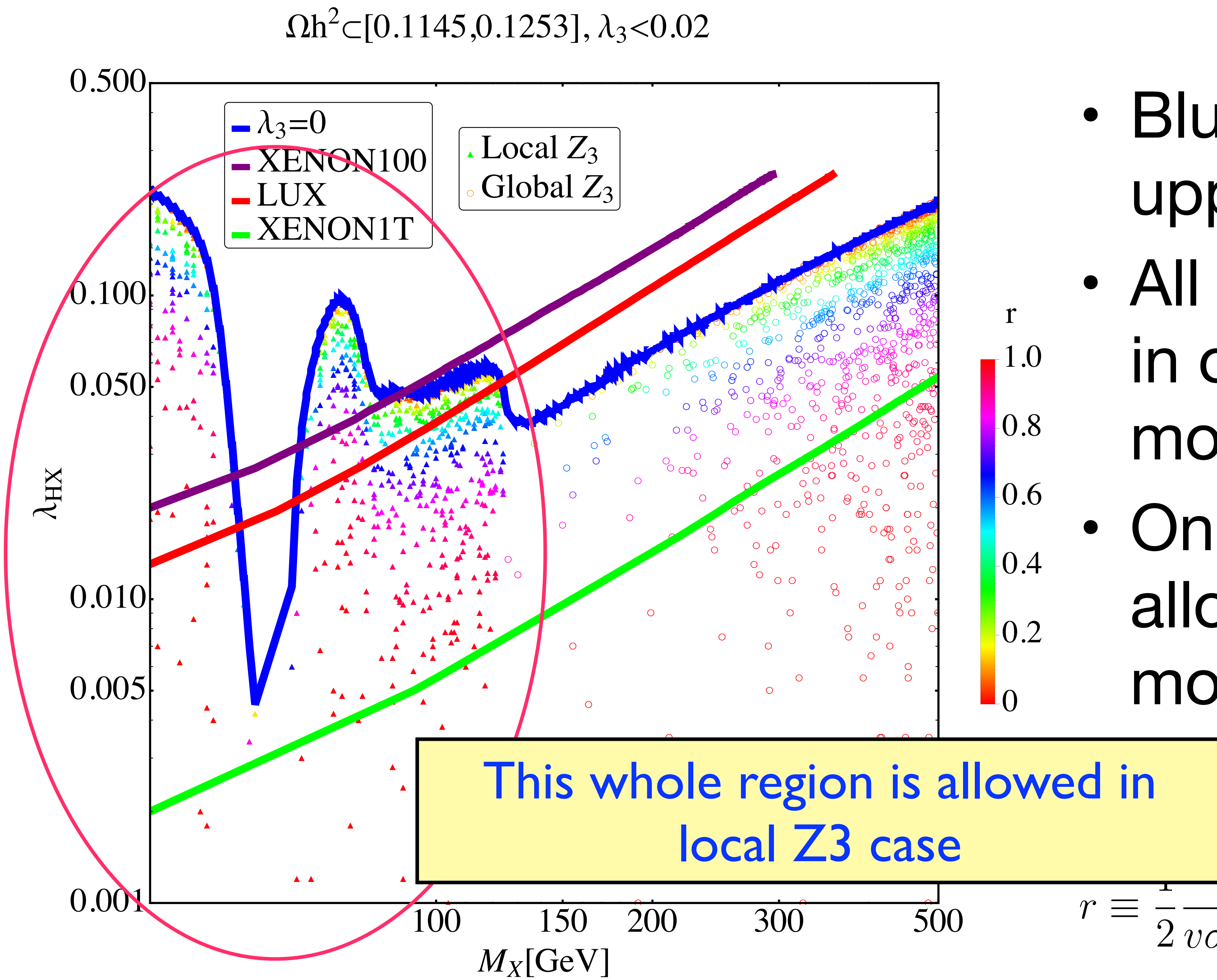

- Blue band marks the upper bound,
- All points are allowed in our local Z3 model,1402.6449
- Only circles are allowed in global Z3 model,1211.1014

$$r \equiv \frac{1}{2}\frac{v\sigma^{XX\to X^*Y}}{v\sigma^{XX^*\to YY} + \frac{1}{2}v\sigma^{XX\to X^*Y}}.$$

Comparison with EFT

$$U(1)_X \text{ sym}: \quad X^\dagger X H^\dagger H, \ \frac{1}{\Lambda^2}\left(X^\dagger D_\mu X\right)\left(H^\dagger D^\mu H\right), \ \frac{1}{\Lambda^2}\left(X^\dagger D_\mu X\right)\left(\overline{f}\gamma^\mu f\right), \ etc. \tag{4.3}$$

$$Z_3 \text{ sym}: \quad \frac{1}{\Lambda}X^3 H^\dagger H, \quad \frac{1}{\Lambda^2}X^3\overline{f}f, \ etc. \tag{4.4}$$

$$\left(\text{or } \frac{1}{\Lambda^3}X^3\overline{f_L}Hf_R, \text{if we imposed the full SM gauge symmetry}\right) \tag{4.5}$$

- There is no Z', H2 in the EFT, and so indirect detection or thermal relic density calculations can be completely different
- Complementarity breaks down : (4.3) cannot capture semi-annihilation

Strong DM self interaction from Light Mediators

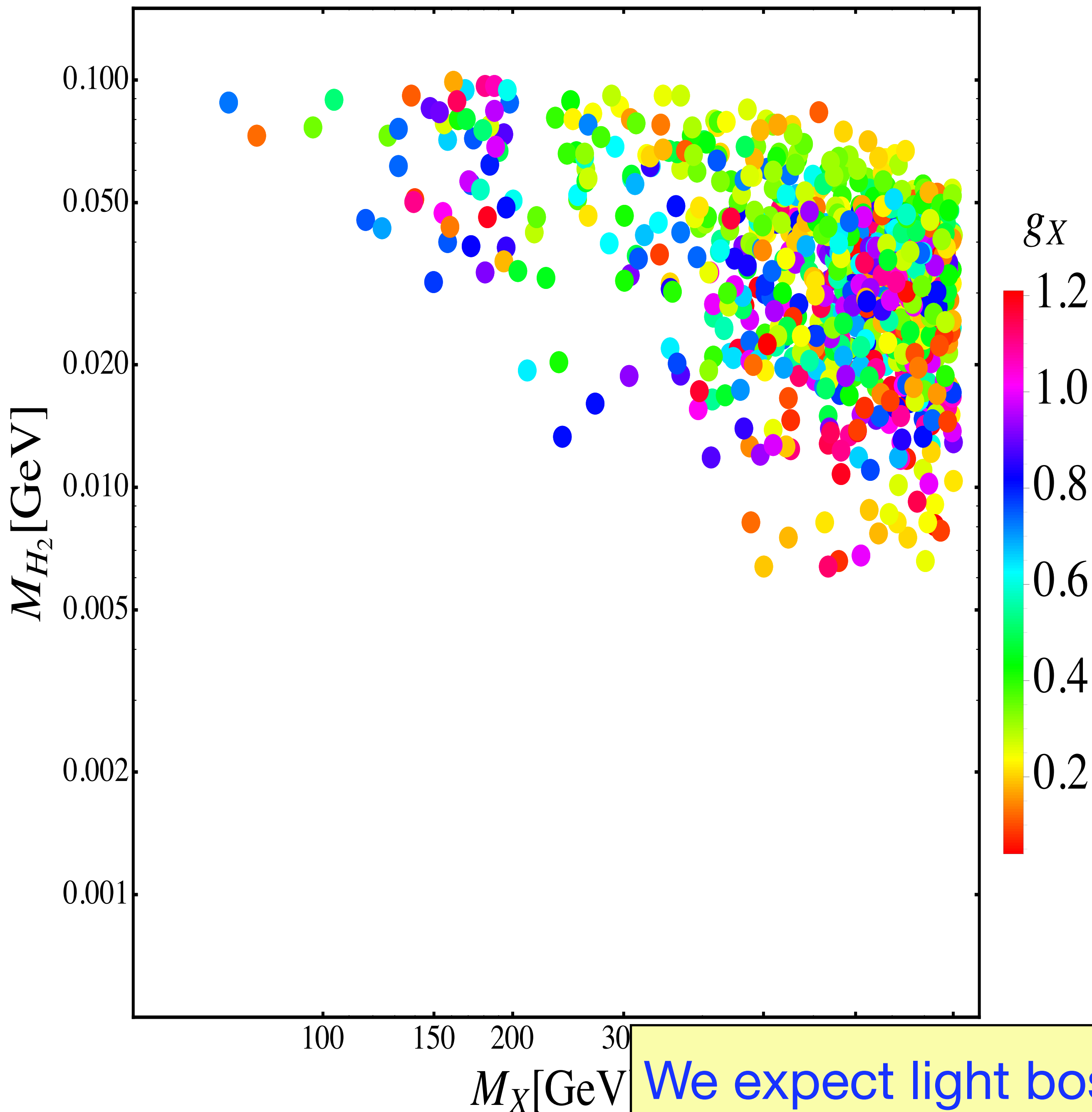

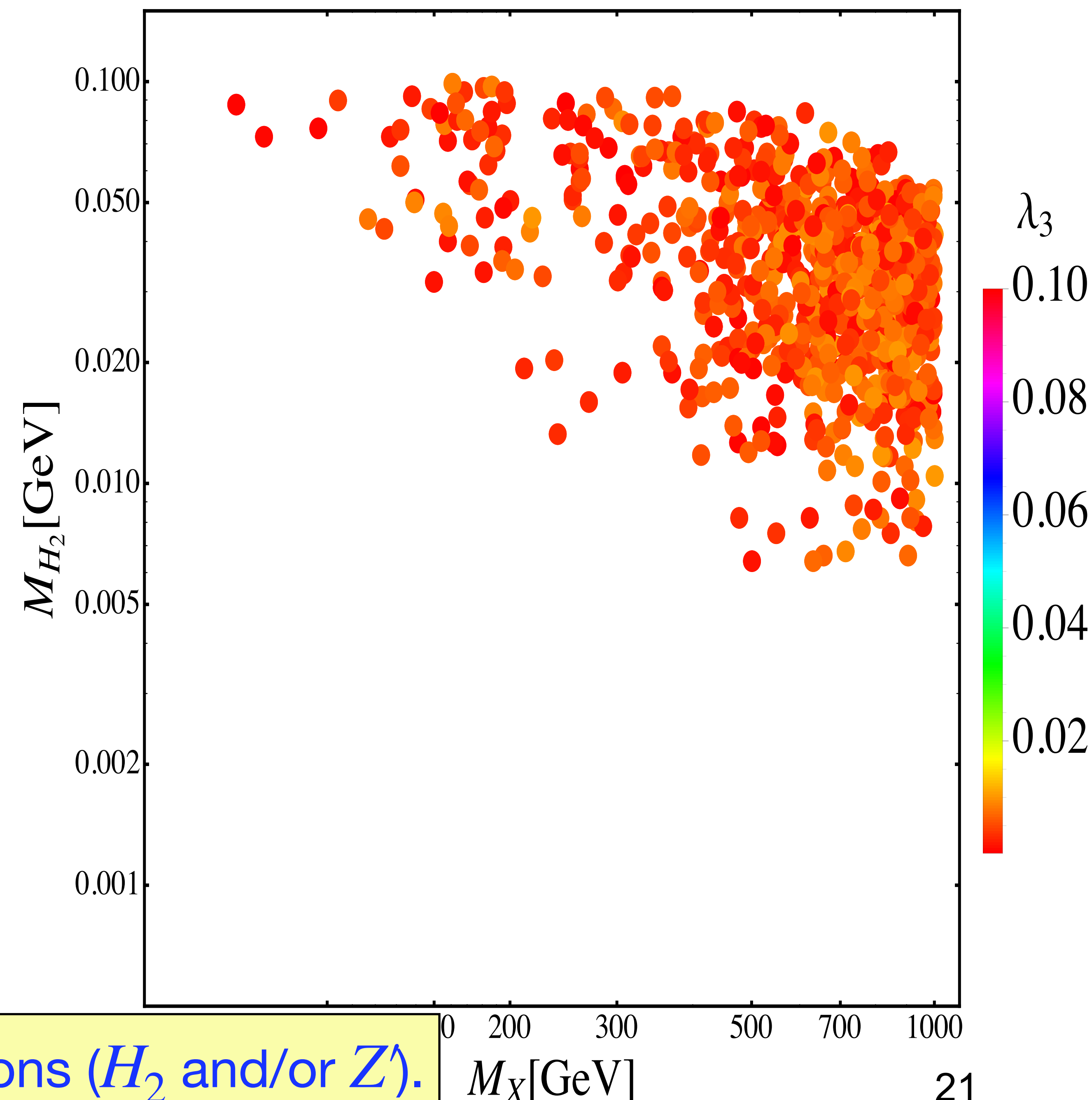

We expect light bosons (H_2 and/or Z').
Can we find them experimentally ?

Galactic center γ-ray excess

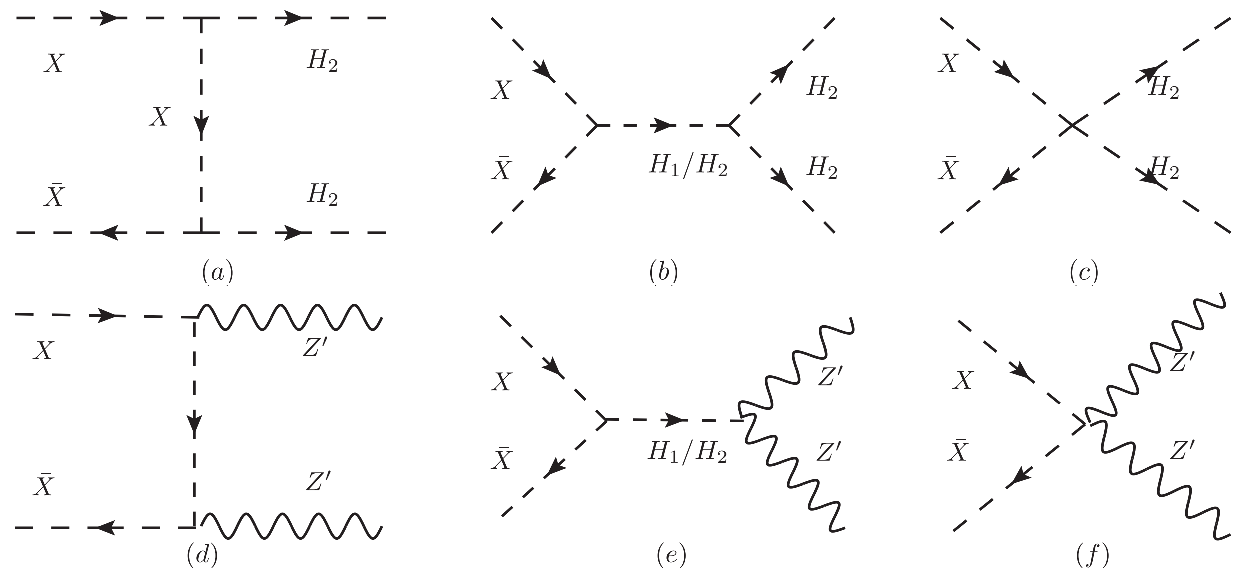

FIG. 1: Feynman diagrams for $X\bar{X}$ annihilation into H_2 and Z'.

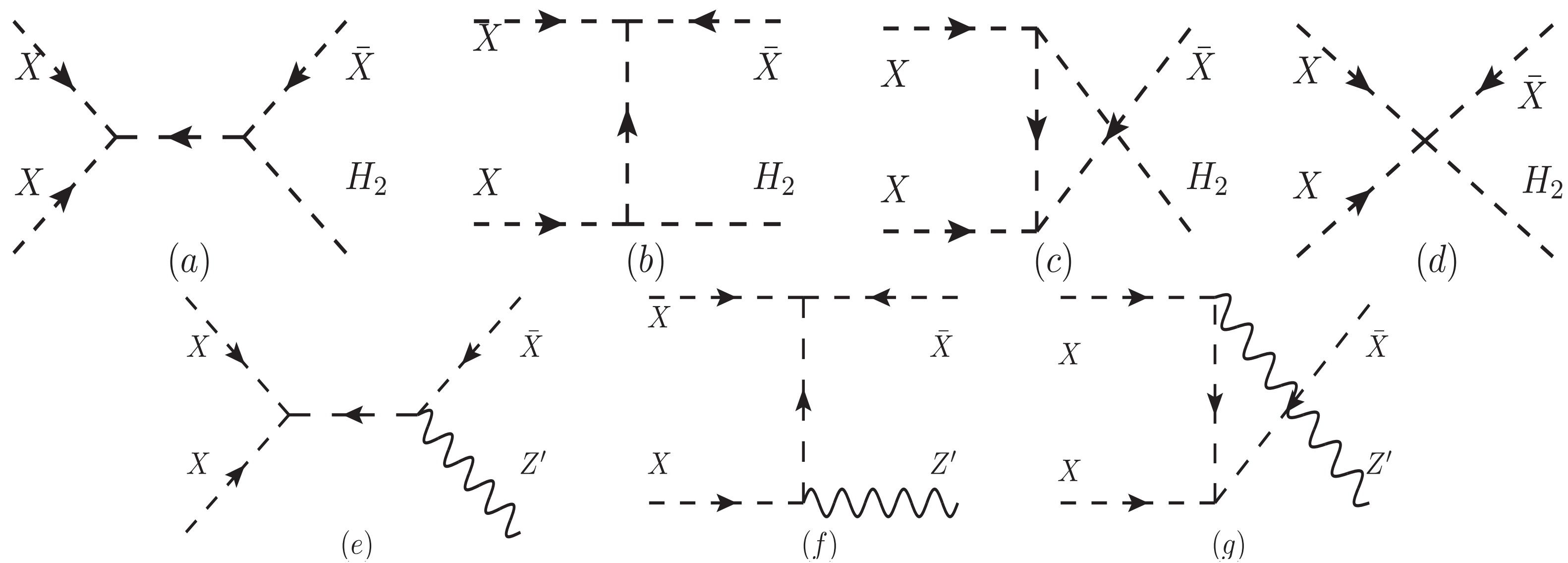

FIG. 2: Feynman diagrams for XX semi-annihilation into H_2 and Z'.

(arXiv:1407.5492 with Yong Tang)

Galactic center γ-ray excess

(arXiv:1407.5492 with Yong Tang)

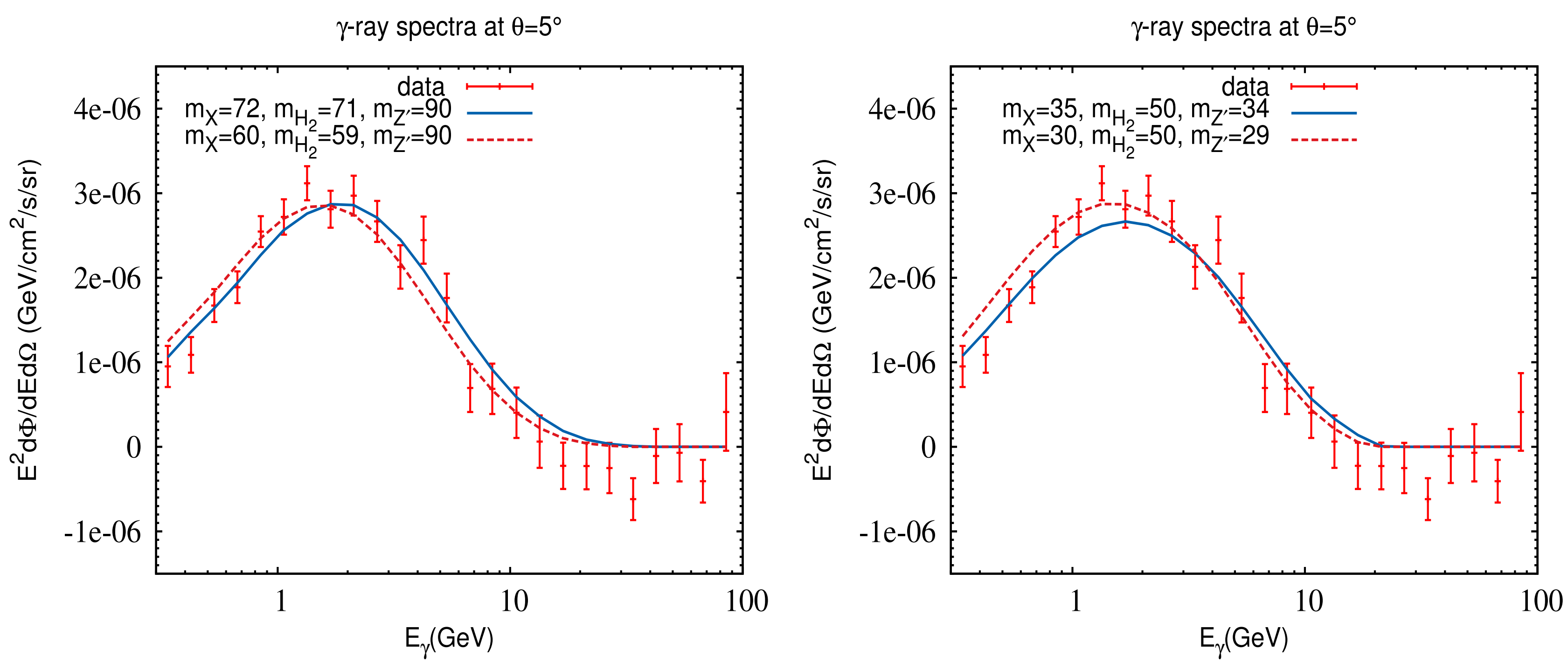

FIG. 4: γ-ray spectra from dark matter (semi-)annihilation with H_2(left) and Z'(right) as final states. In each case, mass of H_2 or Z' is chosen to be close to m_X to avoid large lorentz boost. Masses are in GeV unit. Data points at $\theta = 5$ degree are extracted from [1].

Possible only in local Z_3, not in global Z_3 !!

Inelastic DM models with

$$U(1)_X \to Z_2$$

and XENON1T excess

Based on
- S.Baek, P. Ko, W.I. Park, 1407.6588
- P. Ko, T. Matsui, Y.-L.Tang, 1910.04311
- S.Baek, J.Kim, P. Ko, 2006.16876

Motivations for XDM

- In the usual real scalar DM with Z_2 symmetry, DM stability is not guaranteed in the presence of high dim op's induced by gravity effects
- Better to have local gauge symmetry for absolutely stable DM (Baek,Ko,Park,arXiv:1303.4280)
- Then XDM appears quite naturally $U(1) \to Z_2$ for both scalar and fermion DM cases
- XDM : elementary or composite (dark mesons/baryons/atom…)
- NB : complex scalar DM for $U(1) \to Z_3$ [Ko, Tang, hep-ph:1402.6449, JCAP ; hep-ph:1407.5492, JCAP]

Motivations for XDM

- XDM : phenomenologically interesting possibility, used for interpretation of DAMA, 511 keV γ-ray & PAMELA e^+ excesses, and XENON1T excess, muon (g-2), etc

- Constraints from DD and Colliders are different

- Co-annihilation could be important for relic density calculations

- Usually the mass difference btw XDM & DM is put in by hand, by dim-2 for scalar and dim-3 for fermions DM cases, and dark photon is introduced

- However such theories are mathematically inconsistent and unitarity will be violated in some channels, when (X)DM couples to dark photon

XENON1T Excess

- Excess between 1-7 keV
  - Expectated : 232 ± 15 , Observed : 285
  - Deviation ~ 3.5 σ
- Tritium contamination
  - Long half lifetime (12.3 years)
  - Abundant in atmosphere and cosmogenically produced in Xenon
- Solar axion
  - Produced in the Sun
  - Favored over bkgd @ 3.5 σ
- Neutrino magnetic dipole moment
  - Favored @ 3.2 σ

Electron recoil

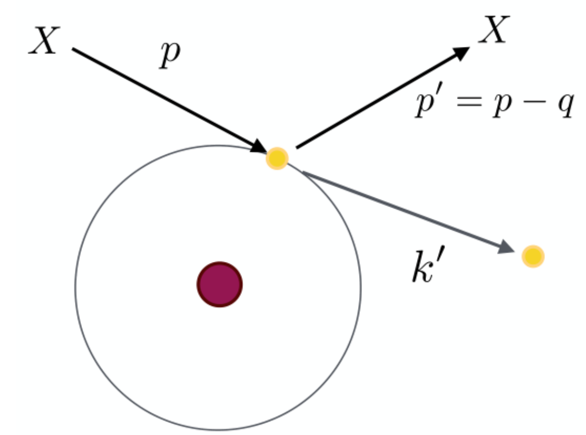

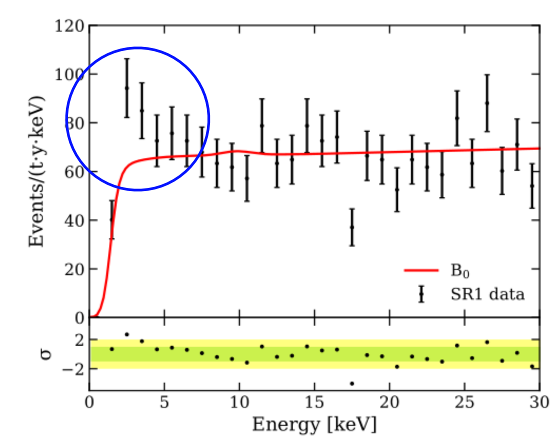

DD/CMB Constraints

- To evade stringent bounds from direct detection expt's : sub GeV DM

- CMB bound excludes thermal DM freeze-out determined by S-wave annihilation : DM annihiliation should be mainly in P-wave $\boxed{\langle \sigma v \rangle \sim \cancel{a} + b v^2}$

Planck 2018
R.K.Leane 35 al, PRD2018

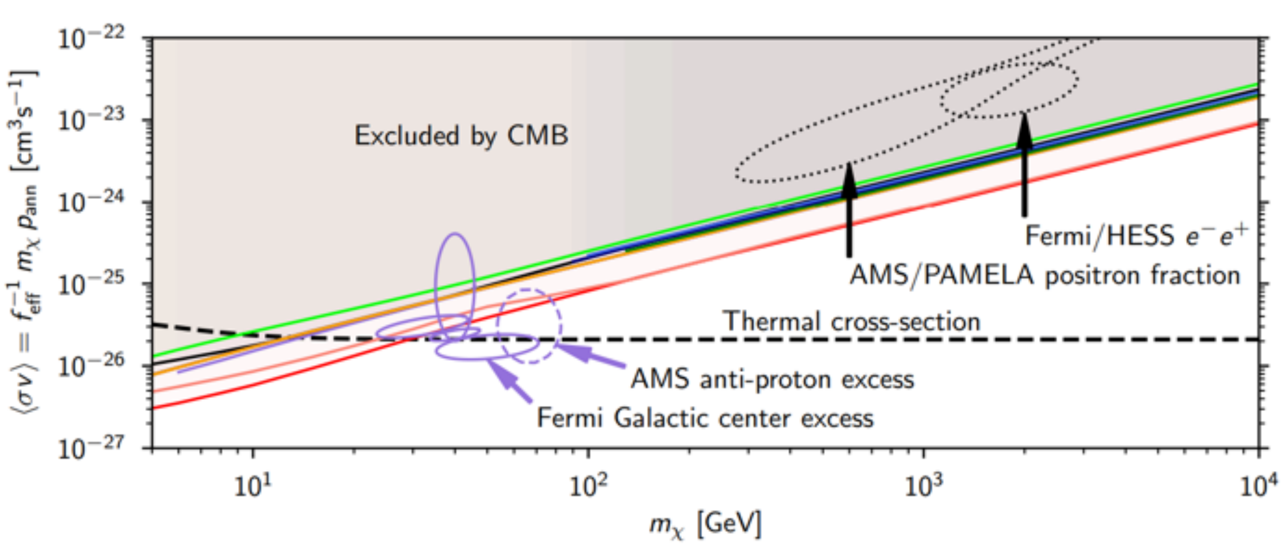

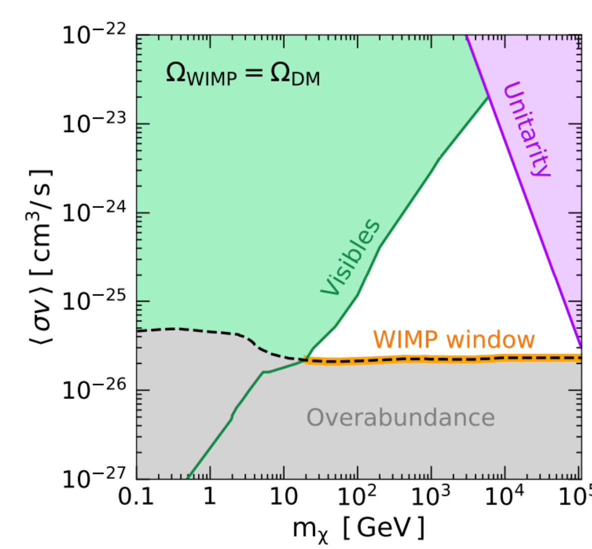

Exothermic DM scattering

- Inelastic exothermic scattering of XDM
- $XDM + e_{\text{atomic}} \to DM + e_{\text{free}}$ by dark photon exchange + kinetic mixing
- Excess is determined by $E_R \sim \delta = m_{XDM} - m_{DM}$
- Most works are based on effective/toy models where δ is put in by hand, or ignored dark Higgs
- dim-2 op for scalar DM and dim-3 op for fermion DM : soft and explicit breaking of local gauge symmetry), and include massive dark photon as well → theoretically inconsistent !

Z_2 DM models with dark Higgs

- We solve this inconsistency and unitarity issue with Krauss-Wilczek mechanism

- By introducing a dark Higgs, we have many advantages:

  - Dark photon gets massive

  - Mass gap δ is generated by dark Higgs mechanism

  - We can have DM pair annihilation in P-wave involving dark Higgs in the final states, unlike in other works

Usual Approaches

For example, Harigaya, Nagai, Suzuki, arXiv:2006.11938

$$V(\phi) = m^2|\phi|^2 + \Delta^2\left(\phi^2 + \phi^{*2}\right), \qquad (1)$$

This term is problematic

$$\mathcal{L} = g_D A'^{\mu}\left(\chi_1\partial_\mu\chi_2 - \chi_2\partial_\mu\chi_1\right) + \epsilon e A'_\mu J^\mu_{\mathrm{EM}},$$

Similarly for the fermion DM case

$\Delta\ \overline{\psi^C}\psi$: breaks U(1) explicitly

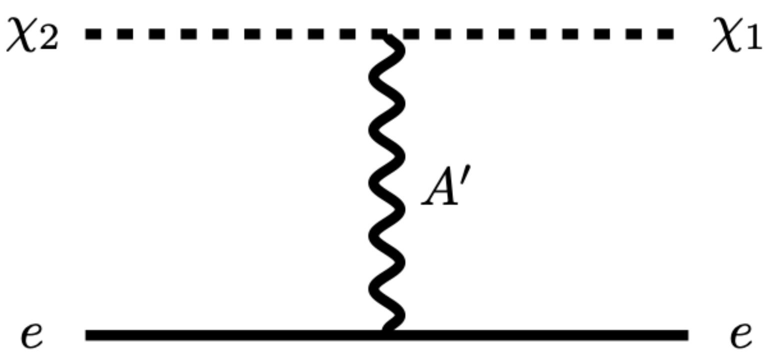

FIG. 1. Inelastic scattering of the heavier DM particle χ_2 off the electron e into the lighter particle χ_1, mediated by the dark photon A'.

- The model is not mathematically consistent, since there is no conserved current a dark photon can couple to in the massless limit
- The second term with Δ^2 breaks $U(1)_X$ explicitly (although softly)

Without dark Higgs

P.Ko, T.Matsui, Yi-Lei Tang, arXiv:1910.04311, Appendix A

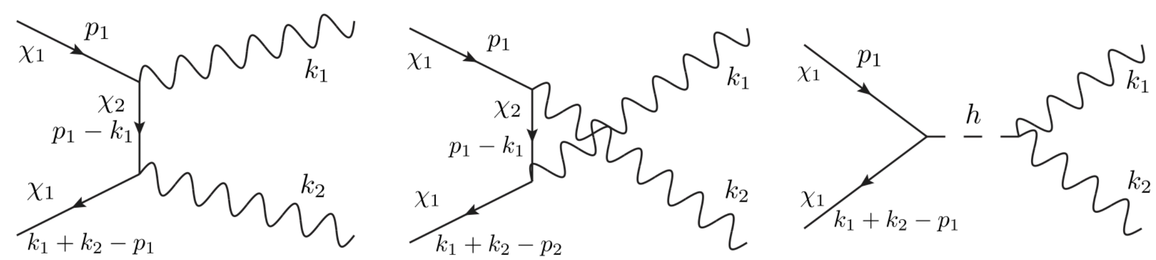

Figure 9: $\chi_1\chi_1 \to \gamma'\gamma'$ diagrams. Compared with the Higgsless soft-breaking model, the third diagram arises in our model

- Only the first two diagrams if the mass gap is given by hand
- The third diagram if the mass gap is generated by dark Higgs mechanism
- Without the last diagram, the amplitude violates unitarity at large $E_{\gamma'}$

Relic Density from

$$XX^{\dagger} \to Z'^{*} \to f\bar{f}$$

(P-wave annihilation)

For example, Harigaya, Nagai, Suzuki, arXiv:2006.11938

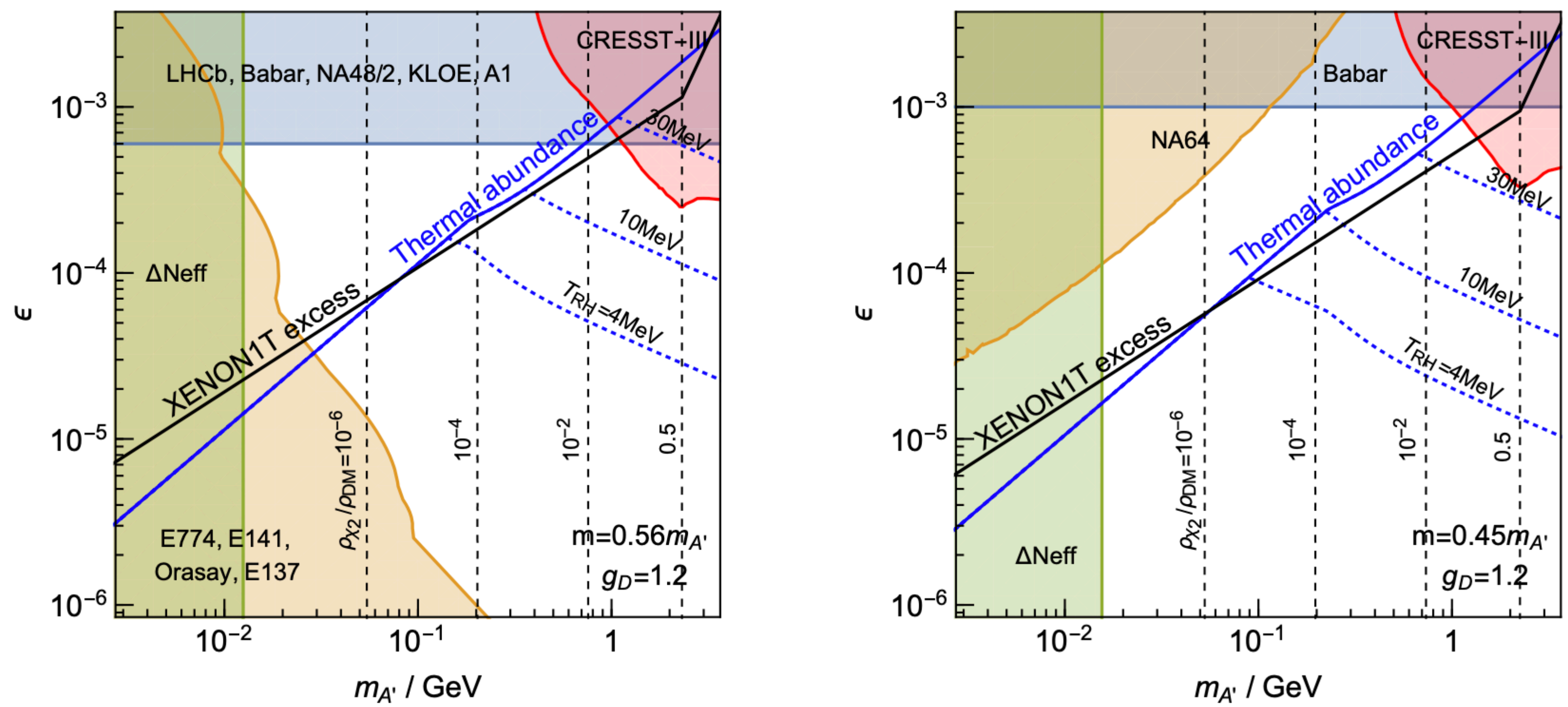

FIG. 4. The required value of ϵ to explain the observed excess of events at XENON1T in terms of the dark photon mass $m_{A'}$ (black solid lines). The left and right panels correspond to the cases of $m > m_{A'}/2$ and $m < m_{A'}/2$ respectively. We assume $g_D = 1.2$ in both cases. The blue lines denote the required value of ϵ to obtain the observed DM abundance by the thermal freeze-out process, discussed in Sec. IV. The solid lines correspond to the case without any entropy production. The dashed lines assume freeze-out during a matter dominated era and the subsequent reheating at $T_{\rm RH}$, which suppresses the DM abundance by a factor of $(T_{\rm RH}/T_{\rm FO})^3$. The black dashed lines denote the mass density of χ_2 normalized by the total DM density. The shaded regions show the constraints from dark radiation and various searches for the dark photon A' which are discussed in Sec. V.

Scalar XDM (X_R & X_I)

Field	ϕ	X	χ
U(1) charge	2	1	1

$$\begin{aligned}\mathcal{L} \;=\; & \mathcal{L}_{\rm SM} - \frac{1}{4}\hat{X}_{\mu\nu}\hat{X}^{\mu\nu} - \frac{1}{2}\sin\epsilon\hat{X}_{\mu\nu}\hat{B}^{\mu\nu} + D^{\mu}\phi^{\dagger}D_{\mu}\phi + D^{\mu}X^{\dagger}D_{\mu}X - m_X^2 X^{\dagger}X + m_{\phi}^2\phi^{\dagger}\phi \\ & -\lambda_{\phi}\left(\phi^{\dagger}\phi\right)^2 - \lambda_X\left(X^{\dagger}X\right)^2 - \lambda_{\phi X}X^{\dagger}X\phi^{\dagger}\phi - \lambda_{\phi H}\phi^{\dagger}\phi H^{\dagger}H - \lambda_{HX}X^{\dagger}XH^{\dagger}H \\ & -\mu\left(X^2\phi^{\dagger} + H.c.\right), \end{aligned} \tag{1}$$

$$X = \frac{1}{\sqrt{2}}(X_R + iX_I),$$

$$H = \begin{pmatrix} 0 \\ \frac{1}{\sqrt{2}}(v_H + h_H)\end{pmatrix}, \quad \phi = \frac{1}{\sqrt{2}}(v_{\phi} + h_{\phi}),$$

$$\mathcal{L} \supset \epsilon g_X s_W Z^{\mu}(X_R\partial_{\mu}X_I - X_I\partial_{\mu}X_R) - \frac{g_Z}{2}Z_{\mu}\overline{\nu}_L\gamma^{\mu}\nu_L.$$

$$\mathcal{L} \supset g_X Z'^{\mu}(X_R\partial_{\mu}X_I - X_I\partial_{\mu}X_R) - \epsilon\, e c_W Z'_{\mu}\overline{e}\gamma^{\mu}e,$$

$U(1) \rightarrow Z_2$ by $v_{\phi} \neq 0 : X \rightarrow -X$

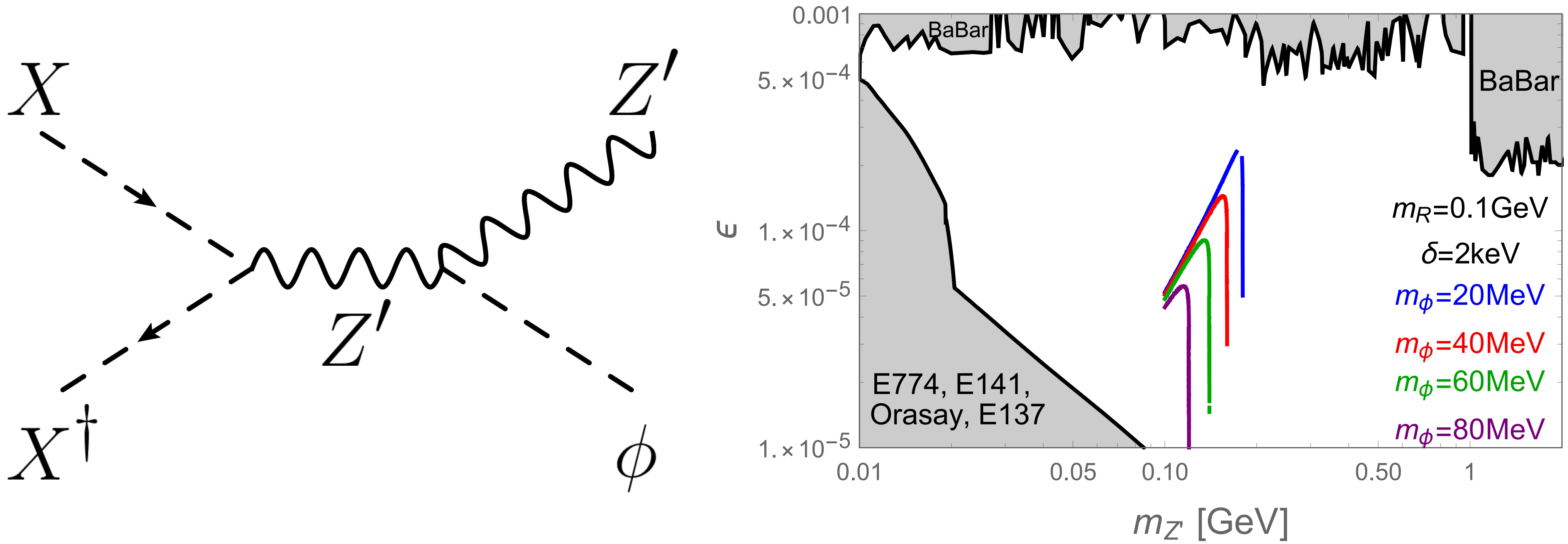

FIG. 1: (*left*) Feynman diagrams relevant for thermal relic density of DM: $XX^\dagger \to Z'\phi$ and (*right*) the region in the $(m_{Z'}, \epsilon)$ plane that is allowed for the XENON1T electron recoil excess and the correct thermal relic density for scalar DM case for $\delta = 2$ keV : (a) $m_{\rm DM} = 0.1$ GeV. Different colors represents $m_\phi = 20, 40, 60, 80$ MeV. The gray areas are excluded by various experiments, from BaBar [61], E774 [62], E141 [63], Orasay [64], and E137 [65], assuming $Z' \to X_R X_I$ is kinematically forbidden.

P-wave annihilation x-sections

Scalar DM : $XX^\dagger \to Z'^* \to Z'\phi$

$$\sigma v \simeq \frac{g_X^4 v^2}{384\pi\, m_X^4 (4m_X^2 - m_{Z'}^2)^2} \left(16m_X^4 + m_{Z'}^4 + m_\phi^4 + 40m_X^2 m_{Z'}^2 - 8m_X^2 m_\phi^2 - 2m_{Z'}^2 m_\phi^2\right)$$
$$\times \left[\left\{4m_X^2 - (m_{Z'} + m_\phi)^2\right\}\left\{4m_X^2 - (m_{Z'} - m_\phi)^2\right\}\right]^{1/2} + \mathcal{O}(v^4), \qquad (10)$$

Fermion XDM (χ_R & χ_I)

$$\mathcal{L} = -\frac{1}{4}\hat{X}^{\mu\nu}\hat{X}_{\mu\nu} - \frac{1}{2}\sin\epsilon\hat{X}_{\mu\nu}B^{\mu\nu} + \overline{\chi}\left(i\not{D} - m_\chi\right)\chi + D_\mu\phi^\dagger D^\mu\phi$$
$$- \mu^2\phi^\dagger\phi - \lambda_\phi|\phi|^4 - \frac{1}{\sqrt{2}}\left(y\phi^\dagger\overline{\chi^C}\chi + \text{h.c.}\right) - \lambda_{\phi H}\phi^\dagger\phi H^\dagger H$$

$$\chi = \frac{1}{\sqrt{2}}(\chi_R + i\chi_I),$$
$$\chi^c = \frac{1}{\sqrt{2}}(\chi_R - i\chi_I),$$
$$\chi_R^c = \chi_R, \quad \chi_I^c = \chi_I,$$

$$\mathcal{L} = \frac{1}{2}\sum_{i=R,I}\overline{\chi_i}\left(i\not{\partial} - m_i\right)\chi_i - i\frac{g_X}{2}(Z'_\mu + \epsilon s_W Z_\mu)\left(\overline{\chi_R}\gamma^\mu\chi_I - \overline{\chi_I}\gamma^\mu\chi_R\right)$$
$$- \frac{1}{2}yh_\phi\left(\overline{\chi_R}\chi_R - \overline{\chi_I}\chi_I\right),$$

$U(1) \to Z_2$ by $v_\phi \neq 0 : \chi \to -\chi$

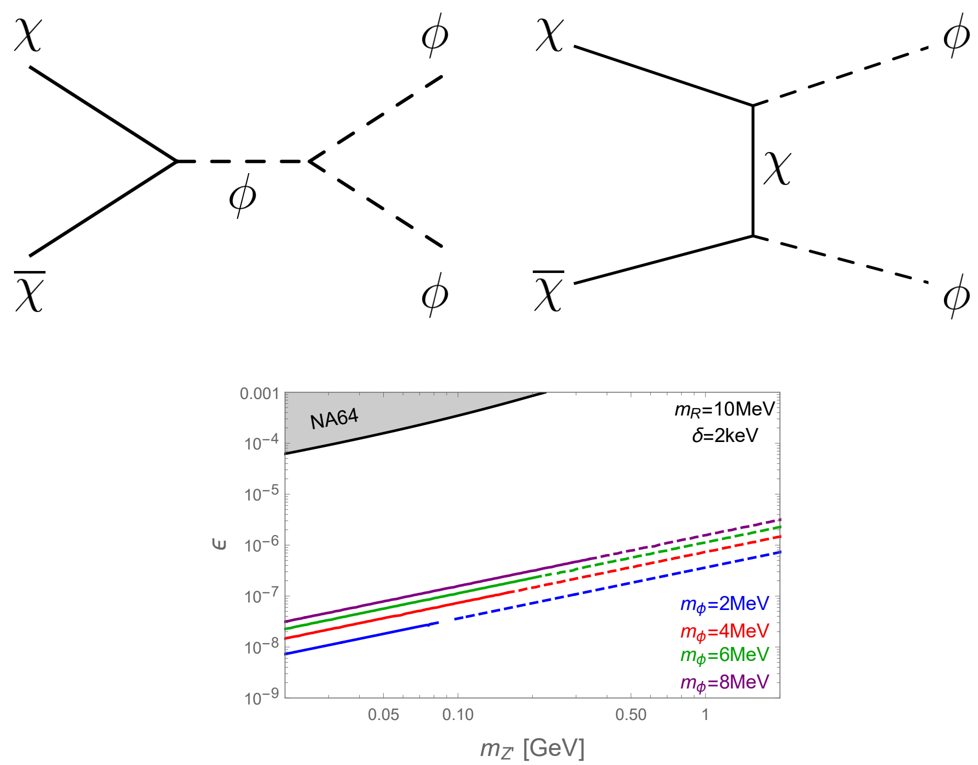

FIG. 2: (*top*) Feyman diagrams for $\chi\bar{\chi} \to \phi\phi$. (*bottom*) the region in the $(m_{Z'}, \epsilon)$ plane that is allowed for the XENON1T electron recoil excess and the correct thermal relic density for fermion DM case for $\delta = 2$ keV and the fermion DM mass to be $m_R = 10$ MeV. Different colors represents $m_\phi = 2, 4, 6, 8$ MeV. The gray areas are excluded by various experiments, assuming $Z' \to \chi_R\chi_I$ is kinematically allowed, and the experimental constraint is weaker in the ϵ we are interested in, compared with the scalar DM case in Fig. 1 (right). We also show the current experimental bounds by NA64 [66].

P-wave annihilation x-sections

Scalar DM : $XX^\dagger \to Z'^* \to Z'\phi$

$$\sigma v \simeq \frac{g_X^4 v^2}{384\pi\, m_X^4 (4m_X^2 - m_{Z'}^2)^2} \left(16 m_X^4 + m_{Z'}^4 + m_\phi^4 + 40 m_X^2 m_{Z'}^2 - 8 m_X^2 m_\phi^2 - 2 m_{Z'}^2 m_\phi^2\right)$$
$$\times \left[\left\{4m_X^2 - (m_{Z'} + m_\phi)^2\right\}\left\{4m_X^2 - (m_{Z'} - m_\phi)^2\right\}\right]^{1/2} + \mathcal{O}(v^4), \qquad (10)$$

Fermion DM : $\chi\overline{\chi} \to \phi\phi$

$$\sigma v = \frac{y^2 v^2 \sqrt{m_\chi^2 - m_\phi^2}}{96\pi m_\chi}\left[\frac{27\lambda_\phi^2 v_\phi^2}{(4m_\chi^2 - m_\phi^2)^2} + \frac{4y^2 m_\chi^2 (9m_\chi^4 - 8m_\chi^2 m_\phi^2 + 2m_\phi^4)}{(2m_\chi^2 - m_\phi^2)^4}\right] + \mathcal{O}(v^4), \qquad (28)$$

Crucial to include "dark Higgs" to have DM pair annihilation in P-wave !!

Determination of
(m, Δm, spin) @ Belle II

arXiv:2101.02503, JHEP
with D.W. Kang, C.-T. Lu

Summary

- Local Z_2 scalar/fermion DM : theoretically well defined & mathematically consistent models for XDM
- Can explain a number of phenomena including the recent XENON1T data
- One can discriminate the spin of (X)DM at Belle II from the polar angle distributions of the decaying points
- DM mass and the Δm can be determined with the focus point method
- Similar studies at ILC, CEPC, HL-LHC and FCC-hh in progress (The current version of FCC CDR does not include this interesting case.)

Multi component SIMP models based on

$$U(1)_X \to Z_2 \times Z_3$$

Based on 2103.05956 (to appear in JHEP)
By Jinsu Kim, P. Ko, J. Li,

Model I : $Z_2(X) \times Z_3(Y)$

TABLE I:

Fields	X	Y	ϕ_X
Charges	$1/2$	$1/3$	1

$$\begin{aligned}
\mathcal{L} &= -\frac{1}{4}X_{\mu\nu}X^{\mu\nu} - \frac{\epsilon}{2}X_{\mu\nu}B^{\mu\nu} + D_\mu X D^\mu X + D_\mu Y D^\mu Y + D_\mu \phi D^\mu \phi \\
&- m_X^2|X|^2 - m_Y^2|Y|^2 - \frac{\lambda_\phi}{4}(|\phi|^2 - v_\phi^2/2)^2 - \frac{\lambda_{X\phi}}{2}|X|^2(|\phi|^2 - v_\phi^2/2) - \frac{\lambda_X}{4}|X|^4 \\
&- \lambda_{Y\phi}|Y|^2(|\phi|^2 - v_\phi/2) - \frac{\lambda_{XH}}{2}|X|^2(|H|^2 - v^2/2) - \frac{\lambda_X}{4}|X|^4 - \lambda_{YH}|Y|^2(|H|^2 - v^2/2) \\
&- \frac{\lambda_{\phi H}}{2}(|\phi|^2 - v_\phi^2/2)(|H|^2 - v^2/2) \qquad (\\
&- \left[\mu_{X\phi}^2\,\phi^\dagger X^2 + \lambda'_{Y\phi}\phi^\dagger\, Y^3 + H.c.\right] \qquad (
\end{aligned}$$

$$\boxed{\begin{aligned} X &\to e^{i\pi}X = -X, \\ Y &\to e^{\pm i2\pi/3}Y. \end{aligned}}$$

Model II : $Z_2(\psi) \times Z_3(Y)$

TABLE II:

Fields	ψ	Y	ϕ_X
Charges	$1/2$	$1/3$	1

$$
\begin{aligned}
\mathcal{L} \;=\; & -\frac{1}{4}X_{\mu\nu}X^{\mu\nu} - \frac{\epsilon}{2}X_{\mu\nu}B^{\mu\nu} + \overline{\psi}(iD\cdot\gamma - m_\psi)\psi + D_\mu Y D^\mu Y + D_\mu\phi D^\mu\phi \\
& - m_Y^2|Y|^2 - \frac{\lambda_\phi}{4}(|\phi|^2 - v_\phi^2/2)^2 - \lambda_{Y\phi}|Y|^2(|\phi|^2 - v_\phi/2) - \lambda_{YH}|Y|^2(|H|^2 - v^2/2) \\
& - \frac{\lambda_{\phi H}}{2}(|\phi|^2 - v_\phi^2/2)(|H|^2 - v^2/2) \\
& - \left[\mu_\phi\phi^\dagger\psi\psi + \lambda'_{Y\phi}\phi^\dagger\, Y^3 + H.c.\right]
\end{aligned}
$$

$$
\boxed{
\begin{aligned}
\psi &\rightarrow e^{i\pi}\psi = -\psi, \\
Y &\rightarrow e^{\pm i2\pi/3}Y.
\end{aligned}
}
$$

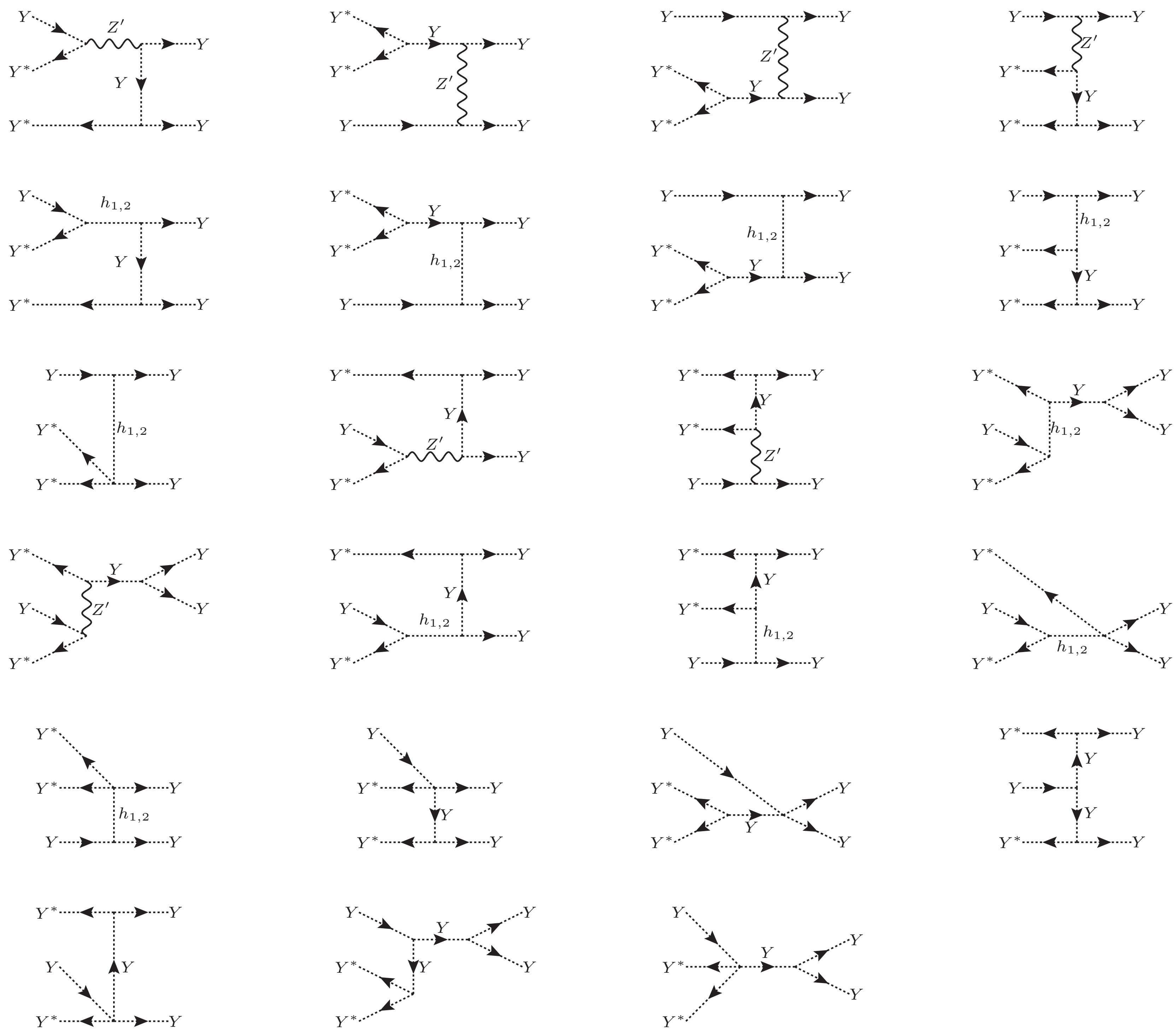

FIG. 1: Feynman diagrams for the process $YY^*Y^* \to YY$ in the case of $m_{X_I} \gg m_Y$ in both Model I and Model II.

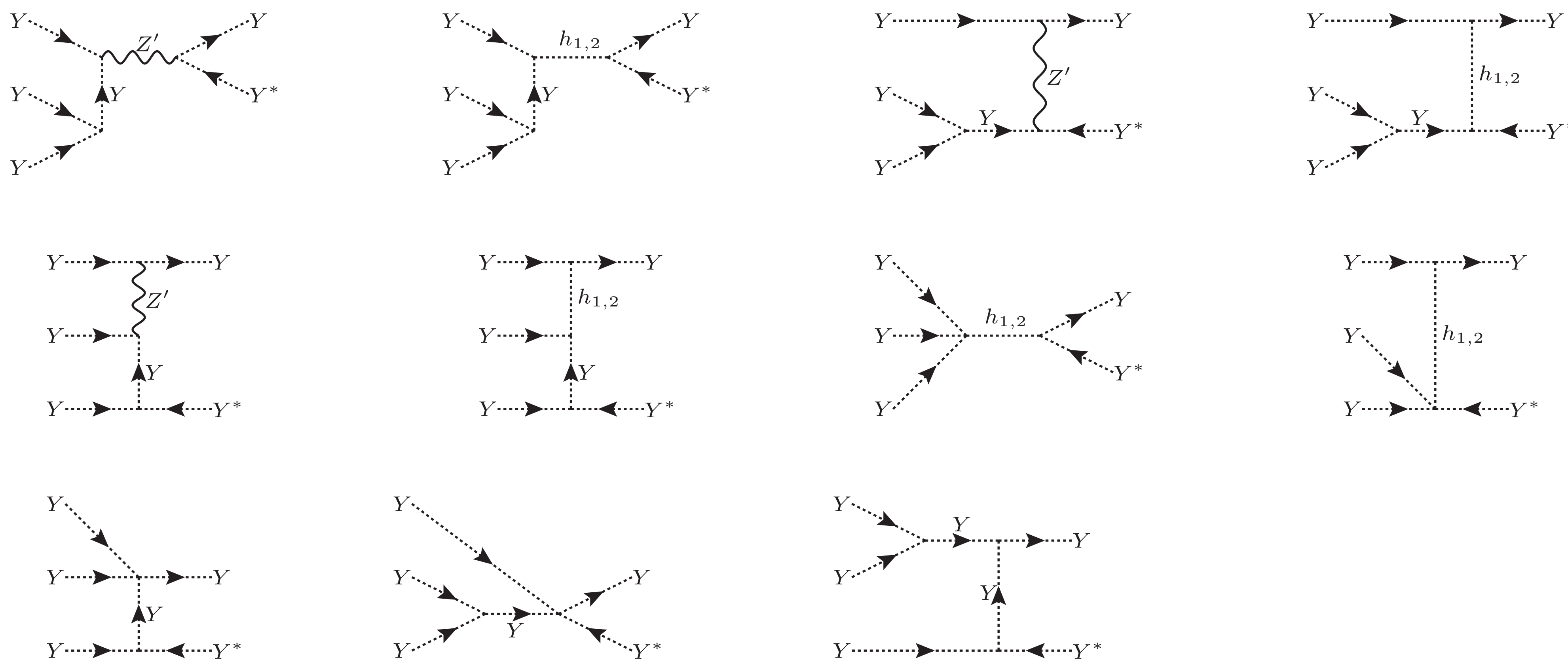

FIG. 2: Feynman diagrams for the process $YYY \to YY^*$ in the case of $m_{X_I} \gg m_Y$ in both Model I and Model II.

General Consideration

- Stability of X and Y : guaranteed by $Z_2 \times Z_3$ (dark charge assignments) even in the presence of nonrenor. op's

- X : scalar (or spin 1/2 fermion), Y : scalar
  Not in this talk

- $\Omega_{\rm DM} \equiv \Omega_{X_I} + \Omega_{X_R} + \Omega_Y$ is determined by the number-changing processes in the dark sector $\longrightarrow$ SIMP model

- Need to keep $XX \to YY^*$ negligible. Otherwise Ω_X will be diluted away into Ω_Y , and not a multi component DM

- Solve Boltzmann Eq's for X_R , X_I , Y , Z'

4 Interesting Scenarios

- 3 DM candidates: Y, X_I, X_R ; 4 different cases

- 2 component scenarios:

  (i) $m_{X_R} \gg m_{X_I} \gg m_Y$, (ii) $m_{X_R} \gg m_{X_I} \sim m_Y$

- 3 component scenarios:

  (iii) $m_{X_R} \sim m_{X_I} \gg m_Y$, (iv) $m_{X_R} \sim m_{X_I} \sim m_Y$

- Inverted mass hierarchy ($m_{X_R} \sim m_{X_I} \ll m_Y$) is not considered

4 Benchmark Points

- Fix : $m_{Z'} = 200$ MeV, $m_{h'} = 30$ GeV, $\lambda_X = 0.025$, $\epsilon = 2 \times 10^{-4}$
- Take λ_{XY} small enough to suppress dilution of Ω_X from $X_i X_i \to YY^*$ $(i = R, I)$

Case	m_{X_R} [MeV]	m_{X_I} [MeV]	m_Y [MeV]	g_X	λ_Y	$\lambda_{Y\phi}$	$\lambda_{X\phi}$	$\lambda'_{Y\phi}$
i)	800	200	50	0.85	6.41	0.9	0.9	0.255
ii)	400	40	37.5	1.3	6.27	1.3	0.5	0.295
iii)	150.01	150	37.5	1.3	5.54	0.05	0.05	0.271
iv)	40.001	40	37.5	1.3	6.27	2.65	2.2	0.295

Table 1. Input parameter values for the four benchmark cases. Cases *i)* and *ii)* correspond to the two-component scenarios and cases *iii)* and *iv)* correspond to the three-component scenarios. We chose $m_{Z'} = 200$ MeV, $m_{h'} = 30$ GeV, $\lambda_X = 0.025$, $\alpha = 10^{-2}$, and $\epsilon = 2 \times 10^{-4}$. Our four benchmark cases are marked as blue points in Figs. 1 and 2.

Constraints

- Perturbativity : $|\lambda_i| < 4\pi$, $\lambda^{'}_{\phi Y} < 4\pi$, $g_X < 4\pi$
- Unitarity : $|\mathscr{M}_{ij\to kl}| < 8\pi$
- Kinetic Equilibrium :
- DM relic density : $\Omega_{\rm DM}h^2 = 0.1200 \pm 0.0012$
- Invisible Higgs decay : $Br(H)_{\rm inv} < 0.19 \longrightarrow \alpha = 10^{-2}$
- $Z^{'}$ searches
- DM self scattering : $0.1\ {\rm cm}^2/{\rm gm} < \dfrac{\sigma_{\rm self}}{m_{\rm DM}} < 10\ {\rm cm}^2/{\rm gm}$

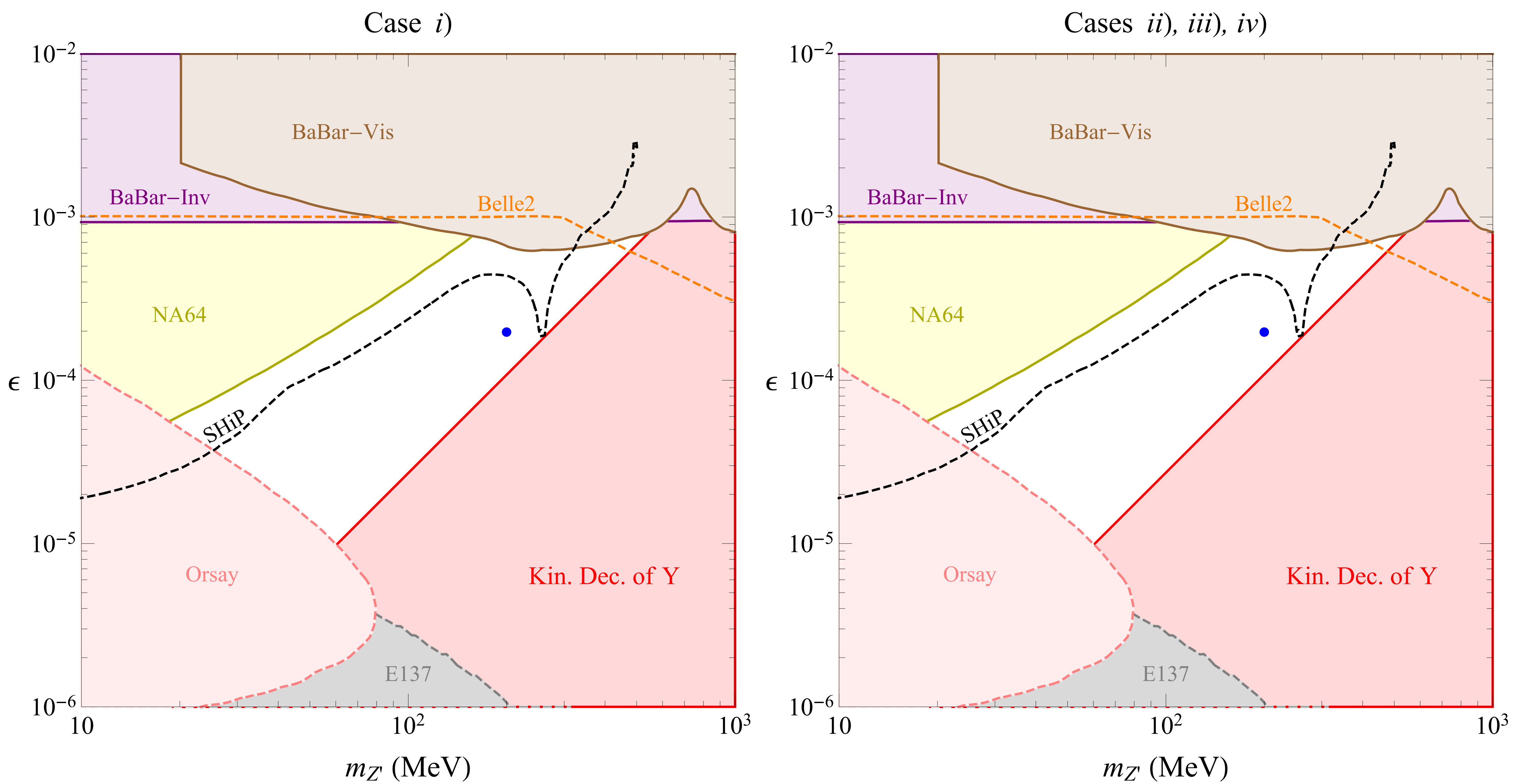

Figure 1. Kinetic decoupling and Z'-search constraints for the case *i)* (left) and cases *ii)*, *iii)*, and *iv)* (right) in the $(m_{Z'}, \epsilon)$ plane. See the main text in Section 3.2 for details of the used constraints. We have the same plot for *ii)*, *iii)*, and *iv)* since the same m_Y, $m_{Z'}$, and ϵ are used. Furthermore, we do not see a clearly visible difference between the left and right plots since the difference in m_Y is small. The blue points represent our benchmark cases shown in Table 1.

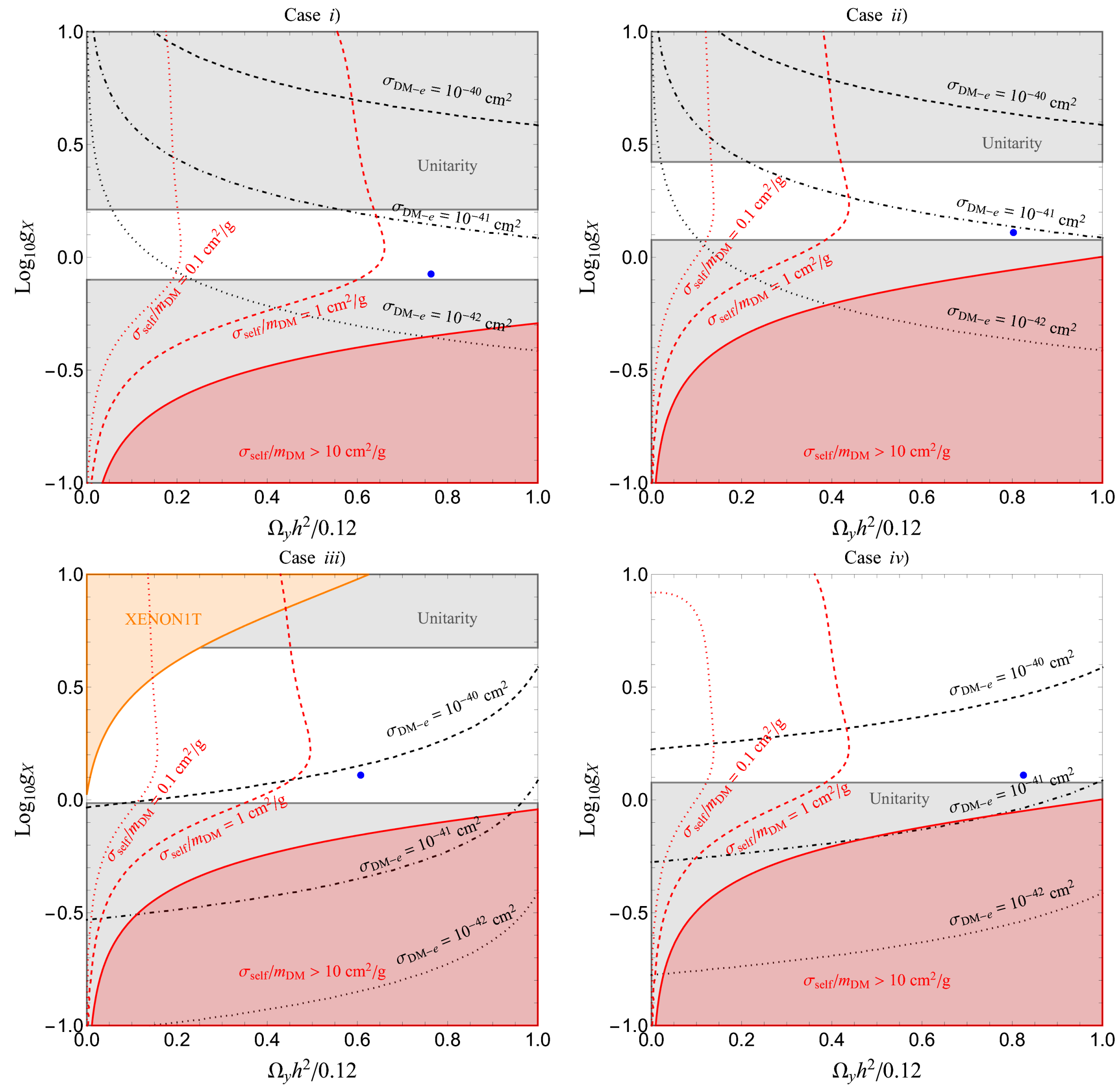

Figure 2. For each case, the unitarity bound (grey), direct detection bound (orange), and large self-scattering cross section bound $\sigma_{\mathrm{self}}/m_{\mathrm{DM}} > 10$ cm^2/g (red) are shown for different values of the dark gauge coupling g_X and the fraction of the Y relic density $\Omega_y h^2/0.12$. The black lines represent DM–electron scattering cross section values, 10^{-40} cm^2 (dashed), 10^{-41} cm^2 (dot-dashed), and 10^{-42} cm^2 (dotted) from top to bottom, respectively. The red lines correspond to two different values of the self-scattering cross section, 0.1 cm^2/g (dotted) and 1 cm^2/g (dashed). For details of the used constraints, see the main text in Section 3.2. The blue points represent our benchmark cases shown in Table 1. Here we vary only g_X and the fraction of the Y relic density, with the condition $(\Omega_y + \Omega_{X_I} + \Omega_{X_R})h^2 = 0.12$. For the two-component DM cases *i)* and *ii)*, $\Omega_{X_R} = 0$ is chosen, while for the three-component DM cases *iii)* and *iv)*, $\Omega_{X_R} = \Omega_{X_I}$ is assumed, except for the self-scattering cross section for which we follow the method outlined in Section 3.2. The other input parameters are fixed (see Table 1). We note that the correct present-day DM relic density constraint is not strictly imposed, except at the benchmark points. Thus, it is important to note that not all the white region is allowed. On the other hand, this approach allows one to comprehensively understand the various constraints and where our benchmark cases lie. The full picture requires an intensive parameter scan by numerically solving the coupled Boltzmann equations which is beyond the scope of the current work.

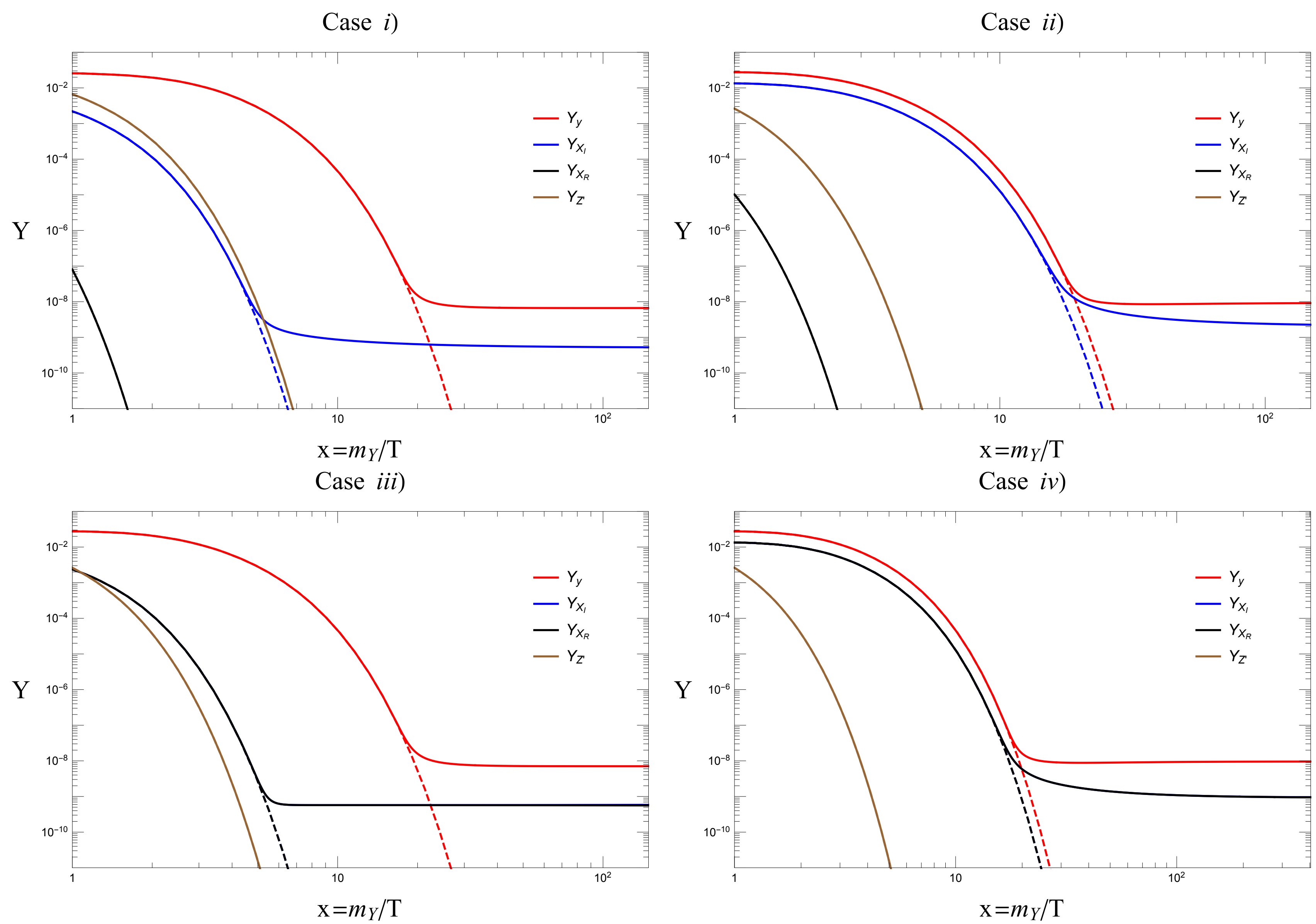

Figure 3. The solutions of the Boltzmann equations summarised in Appendix B are shown for cases *i)–iv)*. The red, blue, black, and brown solid lines are the yields of Y, X_I, X_R, and Z', respectively; here $Y_y \equiv 2Y_Y = 2Y_{Y^*}$. The dashed lines correspond to the equilibrium states. In the cases *i)* and *ii)* Y and X_I relics become frozen out, indicating two-component DM scenarios. On the other hand, in the cases *iii)* and *iv)* all the DM candidates freeze out, and thus we have three-component scenarios. We note that there is no visible difference between the X_I relic and X_R relic in the cases *iii)* and *iv)* due to the small mass gap. A large gauge coupling $g_X \sim \mathcal{O}(1)$ is chosen for our benchmark points. In this case, once the mass gap becomes larger than $\sim$10 keV, a significant amount of the relic of X_R is converted into the X_I relic, mainly through $X_R, Y \to X_I, Y$, becoming a two-component scenario. In all cases we see that Z' follows its equilibrium state.

Case	$\Omega_{X_R}/\Omega_{\rm DM}$	$\Omega_{X_I}/\Omega_{\rm DM}$	$\Omega_y/\Omega_{\rm DM}$	$\sigma_{\rm self}/m_{\rm DM}$ (cm^2/g)	DM scenario
i)	0	0.237	0.763	1.49	Two-component
ii)	0	0.197	0.803	3.83	Two-component
iii)	0.186	0.207	0.607	1.66	Three-component
iv)	0.087	0.088	0.825	4.04	Three-component

Table 2. The fractions of relic density for each DM candidate field and the self-scattering cross sections are shown for the four benchmark cases. The input parameters are summarised in Table 1. The total DM relic density is $\Omega_{\rm DM}h^2 = 0.12$. As expected from the mass gap between X_I and X_R, cases *i)* and *ii)* give rise to two-component DM scenarios, while three-component DM scenarios are realised in the cases *iii)* and *iv)*. The self-scattering cross sections are somewhat larger than 1 cm^2/g imposed by the Bullet Cluster constraint [84–86] (see also Refs. [87, 88] where the similar bound is obtained from cosmological simulations with self-interacting DM), but well within the bound, 10 cm^2/g.

Case	$\frac{m_{X_R}}{m_{X_I}}$	$\frac{m_{X_I}}{m_Y}$	$\lambda'_{Y\phi}$	λ_{XY}	$\frac{\Omega_{X_R}}{\Omega_{\rm DM}}$	$\frac{\Omega_{X_I}}{\Omega_{\rm DM}}$	$\frac{\Omega_y}{\Omega_{\rm DM}}$	$\frac{\sigma_{\rm self}}{m_{\rm DM}}$ (cm^2/g)
i′)	4	4	0.2	0.02	0	0.30	0.70	1.79
ii′)	10	1.07	0.29	0.03	0	0.21	0.79	5.46
iii′)	1.0001	4	0.29	0.04	0.24	0.28	0.48	2.07
iv′)	1.0001	1.07	0.29	0.04	0.09	0.10	0.81	5.74

Table 3. Input parameters with non-zero λ_{XY} and outcomes of DM relics and the self-scattering cross sections. The rest of the input parameters are chosen as follows: $m_Y = 37.5$ MeV, $m_{Z'} = 200$ MeV, $m_{h'} = 10$ GeV, $g_X = 1$, $\lambda_X = 0.1$, $\lambda_{X\phi} = \lambda_{Y\phi} = 10$, and $\lambda_Y = 5$. All the cases are free from the constraints listed in Section 3.2. We see that the multi-component DM scenarios are still realised with sizeable λ_{XY} values. This is due to the destructive interference between the X–Y contact interaction and the dark Higgs mediated processes.

Summary

Summary

- Local Z_2 and Z_3 DM models are interesting and theoretically consistent when dark photon is introduce : They have completely different particle contents and phenomenology

- Local Z_2 model : (i) Consistent model for XDM coupled to dark photon. (ii) Having dark Higgs opens a new window for light DM models without conflict with CMB bounds on the S-wave annihilation, since one can have P-wave annihilation

- Local Z_3 model : Richer phenomenology because of dark photon and dark Higgs (e.g. GC γ-ray excess, SIDM, etc.)

- Dark Higgs : important for unitarity (even for Higgs inflation, with Jinsu Kim, Wan-Il Park, hep-ph/1405.1635, JCAP(2017))

- $U(1)_X \to Z_2 \times Z_3$ DM models are natural setups for multi component DM where DM are stable because of unbroken dark gauge symmetry (WIMP, SIMP, etc..)

- We showed that 2 or 3 components SIMP scenarios can be realized in this setup : different DM species can have vastly different masses (and also different spins)

- The situation is completely different from dark QCD SIMP case, where one can not have vastly different DM masses

- Downside of this type of model : Difficult to verify/falsify by (in)direct DM detections $\to$ Any Good Idea ??

Backup Slides

WIMP with ad hoc Z2 sym

- Global sym. is not enough since

$$-\mathcal{L}_{\rm int} = \begin{cases} \lambda \frac{\phi}{M_{\rm P}} F_{\mu\nu} F \mu\nu & \text{for boson} \\ \lambda \frac{1}{M_{\rm P}} \bar{\psi} \gamma^\mu D_\mu \ell_{Li} H^\dagger & \text{for fermion} \end{cases}$$

Observation requires [M. Ackermann et al. (LAT Collaboration), PRD 86, 022002 (2012)]

$$\tau_{\rm DM} \gtrsim 10^{26-30} {\rm sec} \Rightarrow \begin{cases} m_\phi \lesssim \mathcal{O}(10){\rm keV} \\ m_\psi \lesssim \mathcal{O}(1){\rm GeV} \end{cases}$$

$\Rightarrow$ WIMP is unlikely to be stable

- SM is guided by gauge principle

It looks natural and may need to consider a gauge symmetry in dark sector, too.

Why Dark Symmetry ?

- Is DM absolutely stable or very long lived ?
- If DM is absolutely stable, one can assume it carries a new conserved dark charge, associated with unbroken dark gauge sym
- DM can be long lived (lower bound on DM lifetime is much weaker than that on proton lifetime) if dark sym is spontaneously broken

Higgs is harmful to weak scale DM stability

Z2 sym scalar DM

$$\mathcal{L} = \frac{1}{2}\partial_\mu S \partial^\mu S - \frac{1}{2} m_S^2 S^2 - \frac{\lambda_S}{4!} S^4 - \frac{\lambda_{SH}}{2} S^2 H^\dagger H.$$

- Very popular alternative to SUSY LSP
- Simplest in terms of the # of new dof's
- But, where does this Z2 symmetry come from ?
- Is it Global or Local ?

Fate of CDM with Z2 sym

- Global Z2 cannot save EW scale DM from decay with long enough lifetime

Consider Z_2 breaking operators such as

$$\frac{1}{M_{\rm Planck}} S O_{\rm SM}$$

keeping dim-4 SM operators only

The lifetime of the Z_2 symmetric scalar CDM S is roughly given by

$$\Gamma(S) \sim \frac{m_S{}^3}{M_{\rm Planck}^2} \sim (\frac{m_S}{100 \rm GeV})^3 10^{-37} GeV$$

The lifetime is too short for ~100 GeV DM

Fate of CDM with Z_2 sym

Spontaneously broken local $U(1)_X$ can do the job to some extent, but there is still a problem

Let us assume a local $U(1)_X$ is spontaneously broken by $\langle \phi_X \rangle \neq 0$ with

$$Q_X(\phi_X) = Q_X(X) = 1$$

Then, there are two types of dangerous operators:

$\phi_X^\dagger X H^\dagger H$, and $\phi_X^\dagger X O_{\rm SM}^{(dim-4)}$

Problematic !

Perfectly fine !

- These arguments will apply to DM models based on ad hoc symmetries (Z_2,Z_3 etc.)
- One way out is to implement Z_2 symmetry as local U(1) symmetry (arXiv:1407.6588 with Seungwon Baek and Wan-Il Park);
- See a paper by Ko and Tang on local Z_3 scalar DM, and another by Ko, Omura and Yu on inert 2HDM with local $U(1)_H$
- DM phenomenology richer and DM stability/ longevity on much solider ground

$$Q_X(\phi) = 2, \quad Q_X(X) = 1$$

arXiv:1407.6588 w/ WIPark and SBaek

$$\mathcal{L} = \mathcal{L}_{\rm SM} + -\frac{1}{4}X_{\mu\nu}X^{\mu\nu} - \frac{1}{2}\epsilon X_{\mu\nu}B^{\mu\nu} + D_\mu\phi_X^\dagger D^\mu\phi_X - \frac{\lambda_X}{4}\left(\phi_X^\dagger\phi_X - v_\phi^2\right)^2 + D_\mu X^\dagger D^\mu X - m_X^2 X^\dagger X$$
$$- \frac{\lambda_X}{4}\left(X^\dagger X\right)^2 - \left(\mu X^2\phi^\dagger + H.c.\right) - \frac{\lambda_{XH}}{4}X^\dagger X H^\dagger H - \frac{\lambda_{\phi_X H}}{4}\phi_X^\dagger\phi_X H^\dagger H - \frac{\lambda_{XH}}{4}X^\dagger X\phi_X^\dagger\phi_X$$

The lagrangian is invariant under $X \to -X$ even after $U(1)_X$ symmetry breaking.

Unbroken Local Z2 symmetry

Gauge models for excited DM

$$X_R \to X_I\gamma_h^* \text{ followed by } \gamma_h^* \to \gamma \to e^+e^-$$ **etc.**

The heavier state decays into the lighter state

The local Z2 model is not that simple as the usual Z2 scalar DM model (also for the fermion CDM)

Model Lagrangian

$$q_X(X,\phi) = (1,2)$$

[1407.6588, Seungwon Baek, P. Ko & WIP]

$$\mathcal{L} = \mathcal{L}_{\rm SM} - \frac{1}{4}\hat{X}_{\mu\nu}\hat{X}^{\mu\nu} - \frac{1}{2}\sin\epsilon \hat{X}_{\mu\nu}\hat{B}^{\mu\nu} + D_\mu\phi D^\mu\phi + D_\mu X^\dagger D^\mu X - m_X^2 X^\dagger X + m_\phi^2 \phi^\dagger\phi$$
$$-\lambda_\phi\left(\phi^\dagger\phi\right)^2 - \lambda_X\left(X^\dagger X\right)^2 - \lambda_{\phi X} X^\dagger X \phi^\dagger\phi - \lambda_{\phi H}\phi^\dagger\phi H^\dagger H - \lambda_{HX} X^\dagger X H^\dagger H - \mu\left(X^2\phi^\dagger + H.c.\right).$$

- X : scalar DM (XI and XR, excited DM)
- phi : Dark Higgs
- X_mu : Dark photon
- 3 more fields than Z2 scalar DM model
- Z2 Fermion DM can be worked out too

- Some DM models with Higgs portal

➢ Vector DM with Z2 [1404.5257, P. Ko, WIP & Y. Tang]

$$\mathcal{L}_{VDM} = -\frac{1}{4}X_{\mu\nu}X^{\mu\nu} + (D_\mu\Phi)^\dagger(D^\mu\Phi) - \lambda_\Phi\left(\Phi^\dagger\Phi - \frac{v_\Phi^2}{2}\right)^2$$
$$-\lambda_{\Phi H}\left(\Phi^\dagger\Phi - \frac{v_\Phi^2}{2}\right)\left(H^\dagger H - \frac{v_H^2}{2}\right) ,$$

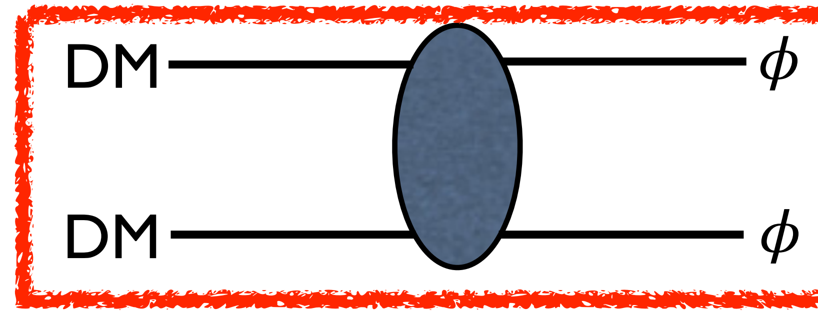

➢ Scalar DM with local Z2 [1407.6588, Seungwon Baek, P. Ko & WIP]

$$\mathcal{L} = \mathcal{L}_{\rm SM} - \frac{1}{4}\hat{X}_{\mu\nu}\hat{X}^{\mu\nu} - \frac{1}{2}\sin\epsilon\hat{X}_{\mu\nu}\hat{B}^{\mu\nu} + D_\mu\phi D^\mu\phi + D_\mu X^\dagger D^\mu X - m_X^2 X^\dagger X + m_\phi^2\phi^\dagger\phi$$
$$-\lambda_\phi\left(\phi^\dagger\phi\right)^2 - \lambda_X\left(X^\dagger X\right)^2 - \lambda_{\phi X}X^\dagger X\phi^\dagger\phi - \lambda_{\phi H}\phi^\dagger\phi H^\dagger H - \lambda_{HX}X^\dagger X H^\dagger H - \mu\left(X^2\phi^\dagger + H.c.\right)$$

- muon (g-2) as well as GeV scale gamma-ray excess explained
- natural realization of excited state of DM
- free from direct detection constraint even for a light Z'

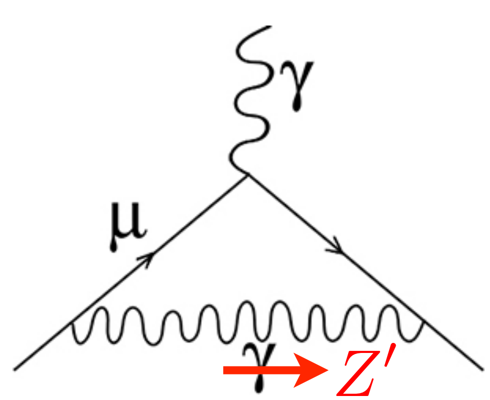

$$\Delta a_\mu \approx \frac{\alpha_{\rm em}\epsilon^2}{2\pi\cos\theta_W^2}$$

$$(\text{for } m_{Z'} \lesssim m_\mu)$$

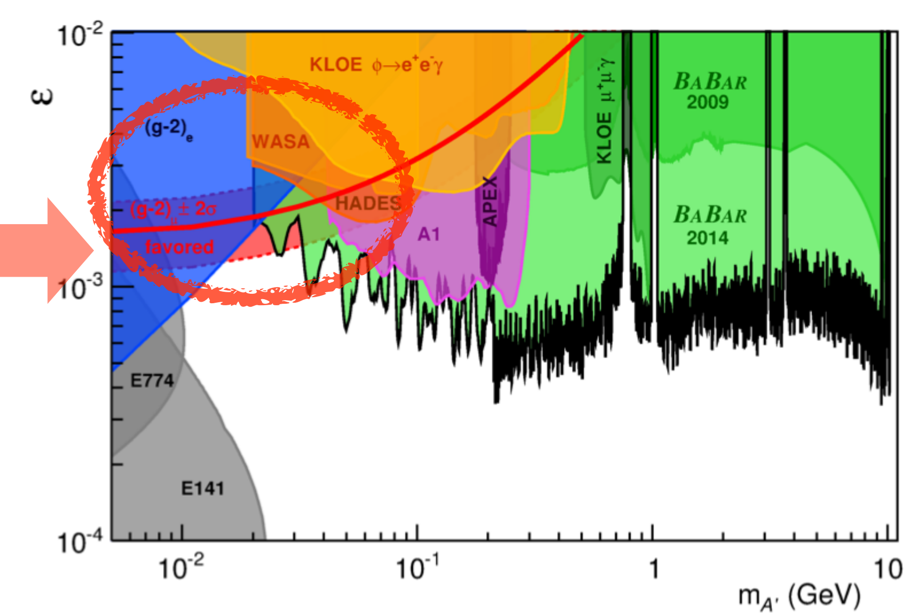

[1406.2980, BaBar collaboration]

Boltzmann Eq's for

$$U(1) \rightarrow Z_2 \times Z_3$$

SIMP DM Models

$$
\begin{aligned}
\frac{dY_y}{dx} = \frac{2x}{H} \Bigg[& \langle\Gamma\rangle_{Z'\to Y,Y^*} \left(Y_{Z'} - \frac{Y_{Z'}^{\rm eq}}{(Y_y^{\rm eq})^2} Y_y^2 \right) + \langle\Gamma\rangle_{X_R\to X_I,Y,Y^*} \left(Y_{X_R} - \frac{Y_{X_R}^{\rm eq}}{Y_{X_I}^{\rm eq}(Y_y^{\rm eq})^2} Y_{X_I} Y_y^2 \right) \Bigg] \\
& + \frac{2s}{Hx^2} \Bigg[\langle\sigma v\rangle_{Z',Z'\to Y,Y^*} \left(Y_{Z'}^2 - \frac{(Y_{Z'}^{\rm eq})^2}{(Y_y^{\rm eq})^2} Y_y^2 \right) + \langle\sigma v\rangle_{X_R,X_R\to Y,Y^*} \left(Y_{X_R}^2 - \frac{(Y_{X_R}^{\rm eq})^2}{(Y_y^{\rm eq})^2} Y_y^2 \right) \\
& + \langle\sigma v\rangle_{X_I,X_I\to Y,Y^*} \left(Y_{X_I}^2 - \frac{(Y_{X_I}^{\rm eq})^2}{(Y_y^{\rm eq})^2} Y_y^2 \right) + \langle\sigma v\rangle_{X_I,X_R\to Y,Y^*} \left(Y_{X_I} Y_{X_R} - \frac{Y_{X_I}^{\rm eq} Y_{X_R}^{\rm eq}}{(Y_y^{\rm eq})^2} Y_y^2 \right) \\
& + \frac{1}{2} \langle\sigma v\rangle_{Z',Y\to Y^*,Y^*} \left(Y_{Z'} Y_y - \frac{Y_{Z'}^{\rm eq}}{Y_y^{\rm eq}} Y_y^2 \right) \Bigg] \\
& + \frac{2s^2}{Hx^5} \Bigg[-\frac{1}{8} \langle\sigma v^2\rangle_{Y,Y,Y^*\to Y^*,Y^*} \left(Y_y^3 - Y_y^{\rm eq} Y_y^2 \right) - \frac{1}{8} \langle\sigma v^2\rangle_{Y,Y,Y\to Y,Y^*} \left(Y_y^3 - Y_y^{\rm eq} Y_y^2 \right) \\
& - \frac{1}{4} \langle\sigma v^2\rangle_{Z',Y,Y^*\to X_I,X_R} \left(Y_{Z'} Y_y^2 - \frac{Y_{Z'}^{\rm eq} (Y_y^{\rm eq})^2}{Y_{X_I}^{\rm eq} Y_{X_R}^{\rm eq}} Y_{X_I} Y_{X_R} \right) - \frac{1}{4} \langle\sigma v^2\rangle_{X_I,Y,Y\to X_I,Y^*} \left(Y_{X_I} Y_y^2 - Y_y^{\rm eq} Y_{X_I} Y_y \right) \\
& - \frac{3}{8} \langle\sigma v^2\rangle_{Y,Y,Y\to X_I,X_R} \left(Y_y^3 - \frac{(Y_y^{\rm eq})^3}{Y_{X_I}^{\rm eq} Y_{X_R}^{\rm eq}} Y_{X_I} Y_{X_R} \right) - \frac{1}{4} \langle\sigma v^2\rangle_{X_I,Y,Y\to X_R,Y^*} \left(Y_{X_I} Y_y^2 - \frac{Y_{X_I}^{\rm eq} Y_y^{\rm eq}}{Y_{X_R}^{\rm eq}} Y_{X_R} Y_y \right) \\
& + \frac{1}{2} \langle\sigma v^2\rangle_{X_I,X_I,Y\to Y^*,Y^*} \left(Y_{X_I}^2 Y_y - \frac{(Y_{X_I}^{\rm eq})^2}{Y_y^{\rm eq}} Y_y^2 \right) - \frac{1}{4} \langle\sigma v^2\rangle_{X_R,Y,Y^*\to Z',X_I} \left(Y_{X_R} Y_y^2 - \frac{Y_{X_R}^{\rm eq} (Y_y^{\rm eq})^2}{Y_{Z'}^{\rm eq} Y_{X_I}^{\rm eq}} Y_{Z'} Y_{X_I} \right) \\
& - \frac{1}{4} \langle\sigma v^2\rangle_{X_R,Y,Y\to X_I,Y^*} \left(Y_{X_R} Y_y^2 - \frac{Y_{X_R}^{\rm eq} Y_y^{\rm eq}}{Y_{X_I}^{\rm eq}} Y_{X_I} Y_y \right) - \frac{3}{8} \langle\sigma v^2\rangle_{Y,Y,Y\to X_R,X_R} \left(Y_y^3 - \frac{(Y_y^{\rm eq})^3}{(Y_{X_R}^{\rm eq})^2} Y_{X_R}^2 \right) \\
& - \frac{1}{4} \langle\sigma v^2\rangle_{X_R,Y,Y\to X_R,Y^*} \left(Y_{X_R} Y_y^2 - Y_y^{\rm eq} Y_{X_R} Y_y \right) + \frac{1}{2} \langle\sigma v^2\rangle_{X_I,X_R,Y\to Y^*,Y^*} \left(Y_{X_I} Y_{X_R} Y_y - \frac{Y_{X_I}^{\rm eq} Y_{X_R}^{\rm eq}}{Y_y^{\rm eq}} Y_y^2 \right) \\
& - \frac{1}{4} \langle\sigma v^2\rangle_{Z',Y,Y^*\to X_I,X_I} \left(Y_{Z'} Y_y^2 - \frac{Y_{Z'}^{\rm eq} (Y_y^{\rm eq})^2}{(Y_{X_I}^{\rm eq})^2} Y_{X_I}^2 \right) - \frac{3}{8} \langle\sigma v^2\rangle_{Y,Y,Y\to X_I,X_I} \left(Y_y^3 - \frac{(Y_y^{\rm eq})^3}{(Y_{X_I}^{\rm eq})^2} Y_{X_I}^2 \right) \\
& + \frac{1}{2} \langle\sigma v^2\rangle_{Z',Z',Y^*\to Y,Y} \left(Y_{Z'}^2 Y_y - \frac{(Y_{Z'}^{\rm eq})^2}{Y_y^{\rm eq}} Y_y^2 \right) + \frac{1}{2} \langle\sigma v^2\rangle_{X_R,X_R,Y\to Y^*,Y^*} \left(Y_{X_R}^2 Y_y - \frac{(Y_{X_R}^{\rm eq})^2}{Y_y^{\rm eq}} Y_y^2 \right) \\
& - \frac{1}{4} \langle\sigma v^2\rangle_{Z',Y^*,Y^*\to Z',Y} \left(Y_{Z'} Y_y^2 - Y_y^{\rm eq} Y_{Z'} Y_y \right) - \frac{1}{4} \langle\sigma v^2\rangle_{Z',Y,Y^*\to X_R,X_R} \left(Y_{Z'} Y_y^2 - \frac{Y_{Z'}^{\rm eq} (Y_y^{\rm eq})^2}{(Y_{X_R}^{\rm eq})^2} Y_{X_R}^2 \right) \\
& + \langle\sigma v^2\rangle_{Z',Z',Z'\to Y,Y^*} \left(Y_{Z'}^3 - \frac{(Y_{Z'}^{\rm eq})^3}{(Y_y^{\rm eq})^2} Y_y^2 \right) + \langle\sigma v^2\rangle_{Z',X_I,X_R\to Y,Y^*} \left(Y_{Z'} Y_{X_I} Y_{X_R} - \frac{Y_{Z'}^{\rm eq} Y_{X_I}^{\rm eq} Y_{X_R}^{\rm eq}}{(Y_y^{\rm eq})^2} Y_y^2 \right) \\
& + \langle\sigma v^2\rangle_{Z',X_R,X_R\to Y,Y^*} \left(Y_{Z'} Y_{X_R}^2 - \frac{Y_{Z'}^{\rm eq} (Y_{X_R}^{\rm eq})^2}{(Y_y^{\rm eq})^2} Y_y^2 \right) + \langle\sigma v^2\rangle_{Z',X_I,X_I\to Y,Y^*} \left(Y_{Z'} Y_{X_I}^2 - \frac{Y_{Z'}^{\rm eq} (Y_{X_I}^{\rm eq})^2}{(Y_y^{\rm eq})^2} Y_y^2 \right) \Bigg].
\end{aligned}
\tag{B.1}
$$

$$
\begin{aligned}
\frac{dY_{X_I}}{dx} = \frac{x}{H}\Bigg[& \langle\Gamma\rangle_{X_R\to Z',X_I}\left(Y_{X_R} - \frac{Y^{\text{eq}}_{X_R}}{Y^{\text{eq}}_{Z'}Y^{\text{eq}}_{X_I}}Y_{Z'}Y_{X_I}\right) + \langle\Gamma\rangle_{Z'\to X_I,X_R}\left(Y_{Z'} - \frac{Y^{\text{eq}}_{Z'}}{Y^{\text{eq}}_{X_I}Y^{\text{eq}}_{X_R}}Y_{X_I}Y_{X_R}\right) \\
& + \langle\Gamma\rangle_{X_R\to X_I,Y,Y^*}\left(Y_{X_R} - \frac{Y^{\text{eq}}_{X_R}}{Y^{\text{eq}}_{X_I}(Y^{\text{eq}}_y)^2}Y_{X_I}Y_y^2\right)\Bigg] \\
& + \frac{s}{Hx^2}\Bigg[2\langle\sigma v\rangle_{Z',Z'\to X_I,X_I}\left(Y_{Z'}^2 - \frac{(Y^{\text{eq}}_{Z'})^2}{(Y^{\text{eq}}_{X_I})^2}Y_{X_I}^2\right) + 2\langle\sigma v\rangle_{X_R,X_R\to X_I,X_I}\left(Y_{X_R}^2 - \frac{(Y^{\text{eq}}_{X_R})^2}{(Y^{\text{eq}}_{X_I})^2}Y_{X_I}^2\right) \\
& + \langle\sigma v\rangle_{X_R,Y\to X_I,Y}\left(Y_{X_R}Y_y - \frac{Y^{\text{eq}}_{X_R}}{Y^{\text{eq}}_{X_I}}Y_{X_I}Y_y\right) - 2\langle\sigma v\rangle_{X_I,X_I\to Z',Z'}\left(Y_{X_I}^2 - \frac{(Y^{\text{eq}}_{X_I})^2}{(Y^{\text{eq}}_{Z'})^2}Y_{Z'}^2\right) \\
& - 2\langle\sigma v\rangle_{X_I,X_I\to Y,Y^*}\left(Y_{X_I}^2 - \frac{(Y^{\text{eq}}_{X_I})^2}{(Y^{\text{eq}}_y)^2}Y_y^2\right) - \langle\sigma v\rangle_{X_I,X_R\to Y,Y^*}\left(Y_{X_I}Y_{X_R} - \frac{Y^{\text{eq}}_{X_I}Y^{\text{eq}}_{X_R}}{(Y^{\text{eq}}_y)^2}Y_y^2\right)\Bigg] \\
& + \frac{s^2}{Hx^5}\Bigg[-\langle\sigma v^2\rangle_{Z',X_I,X_R\to Z',Z'}\left(Y_{Z'}Y_{X_I}Y_{X_R} - \frac{Y^{\text{eq}}_{X_I}Y^{\text{eq}}_{X_R}}{Y^{\text{eq}}_{Z'}}Y_{Z'}^2\right) - \langle\sigma v^2\rangle_{X_I,X_R,Y\to Z',Y}\left(Y_{X_I}Y_{X_R}Y_y - \frac{Y^{\text{eq}}_{X_I}Y^{\text{eq}}_{X_R}}{Y^{\text{eq}}_{Z'}}Y_{Z'}\right. \\
& + \frac{1}{4}\langle\sigma v^2\rangle_{Z',Y,Y^*\to X_I,X_R}\left(Y_{Z'}Y_y^2 - \frac{Y^{\text{eq}}_{Z'}(Y^{\text{eq}}_y)^2}{Y^{\text{eq}}_{X_I}Y^{\text{eq}}_{X_R}}Y_{X_I}Y_{X_R}\right) + \frac{1}{4}\langle\sigma v^2\rangle_{Y,Y,Y\to X_I,X_R}\left(Y_y^3 - \frac{(Y^{\text{eq}}_y)^3}{Y^{\text{eq}}_{X_I}Y^{\text{eq}}_{X_R}}Y_{X_I}Y_{X_R}\right) \\
& - \frac{1}{2}\langle\sigma v^2\rangle_{X_I,Y,Y\to X_R,Y^*}\left(Y_{X_I}Y_y^2 - \frac{Y^{\text{eq}}_{X_I}Y^{\text{eq}}_y}{Y^{\text{eq}}_{X_R}}Y_{X_R}Y_y\right) - 2\langle\sigma v^2\rangle_{X_I,X_I,Y\to Y^*,Y^*}\left(Y_{X_I}^2Y_y - \frac{(Y^{\text{eq}}_{X_I})^2}{Y^{\text{eq}}_y}Y_y^2\right) \\
& + \langle\sigma v^2\rangle_{Z',Z',X_R\to Z',X_I}\left(Y_{Z'}^2Y_{X_R} - \frac{Y^{\text{eq}}_{Z'}Y^{\text{eq}}_{X_R}}{Y^{\text{eq}}_{X_I}}Y_{Z'}Y_{X_I}\right) - \langle\sigma v^2\rangle_{X_I,X_I,X_R\to Z',X_I}\left(Y_{X_I}^2Y_{X_R} - \frac{Y^{\text{eq}}_{X_I}Y^{\text{eq}}_{X_R}}{Y^{\text{eq}}_{Z'}}Y_{Z'}Y_{X_I}\right) \\
& + \langle\sigma v^2\rangle_{X_R,X_R,X_R\to Z',X_I}\left(Y_{X_R}^3 - \frac{(Y^{\text{eq}}_{X_R})^3}{Y^{\text{eq}}_{Z'}Y^{\text{eq}}_{X_I}}Y_{Z'}Y_{X_I}\right) + \frac{1}{4}\langle\sigma v^2\rangle_{X_R,Y,Y^*\to Z',X_I}\left(Y_{X_R}Y_y^2 - \frac{Y^{\text{eq}}_{X_R}(Y^{\text{eq}}_y)^2}{Y^{\text{eq}}_{Z'}Y^{\text{eq}}_{X_I}}Y_{Z'}Y_{X_I}\right) \\
& + \langle\sigma v^2\rangle_{Z',X_I,X_R\to X_I,X_I}\left(Y_{Z'}Y_{X_I}Y_{X_R} - \frac{Y^{\text{eq}}_{Z'}Y^{\text{eq}}_{X_R}}{Y^{\text{eq}}_{X_I}}Y_{X_I}^2\right) + \frac{1}{2}\langle\sigma v^2\rangle_{X_R,Y,Y\to X_I,Y^*}\left(Y_{X_R}Y_y^2 - \frac{Y^{\text{eq}}_{X_R}Y^{\text{eq}}_y}{Y^{\text{eq}}_{X_I}}Y_{X_I}Y_y\right) \\
& - \langle\sigma v^2\rangle_{X_I,X_R,Y\to Y^*,Y^*}\left(Y_{X_I}Y_{X_R}Y_y - \frac{Y^{\text{eq}}_{X_I}Y^{\text{eq}}_{X_R}}{Y^{\text{eq}}_y}Y_y^2\right) - \langle\sigma v^2\rangle_{Z',Z',X_I\to Z',X_R}\left(Y_{Z'}^2Y_{X_I} - \frac{Y^{\text{eq}}_{Z'}Y^{\text{eq}}_{X_I}}{Y^{\text{eq}}_{X_R}}Y_{Z'}Y_{X_R}\right) \\
& - 3\langle\sigma v^2\rangle_{X_I,X_I,X_I\to Z',X_R}\left(Y_{X_I}^3 - \frac{(Y^{\text{eq}}_{X_I})^3}{Y^{\text{eq}}_{Z'}Y^{\text{eq}}_{X_R}}Y_{Z'}Y_{X_R}\right) - \langle\sigma v^2\rangle_{X_I,X_R,X_R\to Z',X_R}\left(Y_{X_I}Y_{X_R}^2 - \frac{Y^{\text{eq}}_{X_I}Y^{\text{eq}}_{X_R}}{Y^{\text{eq}}_{Z'}}Y_{Z'}Y_{X_R}\right) \\
& + \frac{1}{2}\langle\sigma v^2\rangle_{Z',Y,Y^*\to X_I,X_I}\left(Y_{Z'}Y_y^2 - \frac{Y^{\text{eq}}_{Z'}(Y^{\text{eq}}_y)^2}{(Y^{\text{eq}}_{X_I})^2}Y_{X_I}^2\right) + \frac{1}{2}\langle\sigma v^2\rangle_{Y,Y,Y\to X_I,X_I}\left(Y_y^3 - \frac{(Y^{\text{eq}}_y)^3}{(Y^{\text{eq}}_{X_I})^2}Y_{X_I}^2\right) \\
& - \langle\sigma v^2\rangle_{Z',X_I,X_R\to X_R,X_R}\left(Y_{Z'}Y_{X_I}Y_{X_R} - \frac{Y^{\text{eq}}_{Z'}Y^{\text{eq}}_{X_I}}{Y^{\text{eq}}_{X_R}}Y_{X_R}^2\right) - \langle\sigma v^2\rangle_{Z',X_I,Y\to X_R,Y}\left(Y_{Z'}Y_{X_I}Y_y - \frac{Y^{\text{eq}}_{Z'}Y^{\text{eq}}_{X_I}}{Y^{\text{eq}}_{X_R}}Y_{X_R}Y_y\right) \\
& - 2\langle\sigma v^2\rangle_{X_I,X_I,Y\to Z',Y}\left(Y_{X_I}^2Y_y - \frac{(Y^{\text{eq}}_{X_I})^2}{Y^{\text{eq}}_{Z'}}Y_{Z'}Y_y\right) + \langle\sigma v^2\rangle_{Z',Z',Z'\to X_I,X_R}\left(Y_{Z'}^3 - \frac{(Y^{\text{eq}}_{Z'})^3}{Y^{\text{eq}}_{X_I}Y^{\text{eq}}_{X_R}}Y_{X_I}Y_{X_R}\right) \\
& - \langle\sigma v^2\rangle_{Z',X_I,X_I\to X_I,X_R}\left(Y_{Z'}Y_{X_I}^2 - \frac{Y^{\text{eq}}_{Z'}Y^{\text{eq}}_{X_I}}{Y^{\text{eq}}_{X_R}}Y_{X_I}Y_{X_R}\right) + \langle\sigma v^2\rangle_{Z',X_R,X_R\to X_I,X_R}\left(Y_{Z'}Y_{X_R}^2 - \frac{Y^{\text{eq}}_{Z'}Y^{\text{eq}}_{X_R}}{Y^{\text{eq}}_{X_I}}Y_{X_I}Y_{X_R}\right) \\
& + \langle\sigma v^2\rangle_{Z',X_R,Y\to X_I,Y}\left(Y_{Z'}Y_{X_R}Y_y - \frac{Y^{\text{eq}}_{Z'}Y^{\text{eq}}_{X_R}}{Y^{\text{eq}}_{X_I}}Y_{X_I}Y_y\right) - \langle\sigma v^2\rangle_{Z',X_I,X_R\to Y,Y^*}\left(Y_{Z'}Y_{X_I}Y_{X_R} - \frac{Y^{\text{eq}}_{Z'}Y^{\text{eq}}_{X_I}Y^{\text{eq}}_{X_R}}{(Y^{\text{eq}}_y)^2}Y_y^2\right) \\
& - 2\langle\sigma v^2\rangle_{Z',X_I,X_I\to Y,Y^*}\left(Y_{Z'}(Y_{X_I})^2 - \frac{Y^{\text{eq}}_{Z'}(Y^{\text{eq}}_{X_I})^2}{(Y^{\text{eq}}_y)^2}Y_y^2\right)\Bigg],
\end{aligned}
\tag{B.2}
$$

$$
\begin{aligned}
\frac{dY_{X_R}}{dx} = \frac{x}{H}\Bigg[& \langle\Gamma\rangle_{Z'\to X_I,X_R}\left(Y_{Z'}-\frac{Y^{\mathrm{eq}}_{Z'}}{Y^{\mathrm{eq}}_{X_I}Y^{\mathrm{eq}}_{X_R}}Y_{X_I}Y_{X_R}\right)-\langle\Gamma\rangle_{X_R\to Z',X_I}\left(Y_{X_R}-\frac{Y^{\mathrm{eq}}_{X_R}}{Y^{\mathrm{eq}}_{Z'}Y^{\mathrm{eq}}_{X_I}}Y_{Z'}Y_{X_I}\right) \\
& -\langle\Gamma\rangle_{X_R\to X_I,Y,Y^*}\left(Y_{X_R}-\frac{Y^{\mathrm{eq}}_{X_R}}{Y^{\mathrm{eq}}_{X_I}(Y^{\mathrm{eq}}_y)^2}Y_{X_I}Y_y^2\right)\Bigg] \\
& +\frac{s}{Hx^2}\Bigg[2\langle\sigma v\rangle_{Z',Z'\to X_R,X_R}\left(Y_{Z'}^2-\frac{(Y^{\mathrm{eq}}_{Z'})^2}{(Y^{\mathrm{eq}}_{X_R})^2}Y_{X_R}^2\right)-2\langle\sigma v\rangle_{X_R,X_R\to Z',Z'}\left(Y_{X_R}^2-\frac{(Y^{\mathrm{eq}}_{X_R})^2}{(Y^{\mathrm{eq}}_{Z'})^2}Y_{Z'}^2\right) \\
& -2\langle\sigma v\rangle_{X_R,X_R\to X_I,X_I}\left(Y_{X_R}^2-\frac{(Y^{\mathrm{eq}}_{X_R})^2}{(Y^{\mathrm{eq}}_{X_I})^2}Y_{X_I}^2\right)-2\langle\sigma v\rangle_{X_R,X_R\to Y,Y^*}\left(Y_{X_R}^2-\frac{(Y^{\mathrm{eq}}_{X_R})^2}{(Y^{\mathrm{eq}}_{y})^2}Y_{y}^2\right) \\
& -\langle\sigma v\rangle_{X_R,Y\to X_I,Y}\left(Y_{X_R}Y_y-\frac{Y^{\mathrm{eq}}_{X_R}}{Y^{\mathrm{eq}}_{X_I}}Y_{X_I}Y_y\right)-\langle\sigma v\rangle_{X_I,X_R\to Y,Y^*}\left(Y_{X_I}Y_{X_R}-\frac{Y^{\mathrm{eq}}_{X_I}Y^{\mathrm{eq}}_{X_R}}{(Y^{\mathrm{eq}}_{y})^2}Y_{y}^2\right)\Bigg] \\
& +\frac{s^2}{Hx^5}\Bigg[-\langle\sigma v^2\rangle_{Z',X_I,X_R\to Z',Z'}\left(Y_{Z'}Y_{X_I}Y_{X_R}-\frac{Y^{\mathrm{eq}}_{X_I}Y^{\mathrm{eq}}_{X_R}}{Y^{\mathrm{eq}}_{Z'}}Y_{Z'}^2\right)-\langle\sigma v^2\rangle_{X_I,X_R,Y\to Z',Y}\left(Y_{X_I}Y_{X_R}Y_y-\frac{Y^{\mathrm{eq}}_{X_I}Y^{\mathrm{eq}}_{X_R}}{Y^{\mathrm{eq}}_{Z'}}Y_{Z'}Y_y\right. \\
& -2\langle\sigma v^2\rangle_{X_R,X_R,Y\to Z',Y}\left(Y_{X_R}^2Y_y-\frac{(Y^{\mathrm{eq}}_{X_R})^2}{Y^{\mathrm{eq}}_{Z'}}Y_{Z'}Y_y\right)+\frac{1}{4}\langle\sigma v^2\rangle_{Z',Y,Y^*\to X_I,X_R}\left(Y_{Z'}Y_y^2-\frac{Y^{\mathrm{eq}}_{Z'}(Y^{\mathrm{eq}}_y)^2}{Y^{\mathrm{eq}}_{X_I}Y^{\mathrm{eq}}_{X_R}}Y_{X_I}Y_{X_R}\right) \\
& +\frac{1}{4}\langle\sigma v^2\rangle_{Y,Y,Y\to X_I,X_R}\left(Y_y^3-\frac{(Y^{\mathrm{eq}}_y)^3}{Y^{\mathrm{eq}}_{X_I}Y^{\mathrm{eq}}_{X_R}}Y_{X_I}Y_{X_R}\right)+\frac{1}{2}\langle\sigma v^2\rangle_{X_I,Y^*,Y^*\to X_R,Y}\left(Y_{X_I}Y_y^2-\frac{Y^{\mathrm{eq}}_{X_I}Y^{\mathrm{eq}}_y}{Y^{\mathrm{eq}}_{X_R}}Y_{X_R}Y_y\right) \\
& -\langle\sigma v^2\rangle_{Z',Z',X_R\to Z',X_I}\left(Y_{Z'}^2Y_{X_R}-\frac{Y^{\mathrm{eq}}_{Z'}Y^{\mathrm{eq}}_{X_R}}{Y^{\mathrm{eq}}_{X_I}}Y_{Z'}Y_{X_I}\right)-\langle\sigma v^2\rangle_{X_I,X_I,X_R\to Z',X_I}\left(Y_{X_I}^2Y_{X_R}-\frac{Y^{\mathrm{eq}}_{X_I}Y^{\mathrm{eq}}_{X_R}}{Y^{\mathrm{eq}}_{Z'}}Y_{Z'}Y_{X_I}\right) \\
& -3\langle\sigma v^2\rangle_{X_R,X_R,X_R\to Z',X_I}\left(Y_{X_R}^3-\frac{(Y^{\mathrm{eq}}_{X_R})^3}{Y^{\mathrm{eq}}_{Z'}Y^{\mathrm{eq}}_{X_I}}Y_{Z'}Y_{X_I}\right)-\frac{1}{4}\langle\sigma v^2\rangle_{X_R,Y,Y^*\to Z',X_I}\left(Y_{X_R}Y_y^2-\frac{Y^{\mathrm{eq}}_{X_R}(Y^{\mathrm{eq}}_y)^2}{Y^{\mathrm{eq}}_{Z'}Y^{\mathrm{eq}}_{X_I}}Y_{Z'}Y_{X_I}\right) \\
& -\langle\sigma v^2\rangle_{Z',X_I,X_R\to X_I,X_I}\left(Y_{Z'}Y_{X_I}Y_{X_R}-\frac{Y^{\mathrm{eq}}_{Z'}Y^{\mathrm{eq}}_{X_R}}{Y^{\mathrm{eq}}_{X_I}}Y_{X_I}^2\right)-\frac{1}{2}\langle\sigma v^2\rangle_{X_R,Y,Y\to X_I,Y^*}\left(Y_{X_R}Y_y^2-\frac{Y^{\mathrm{eq}}_{X_R}Y^{\mathrm{eq}}_y}{Y^{\mathrm{eq}}_{X_I}}Y_{X_I}Y_y\right) \\
& +\frac{1}{2}\langle\sigma v^2\rangle_{Y,Y,Y\to X_R,X_R}\left(Y_y^3-\frac{(Y^{\mathrm{eq}}_y)^3}{(Y^{\mathrm{eq}}_{X_R})^2}Y_{X_R}^2\right)-\langle\sigma v^2\rangle_{X_I,X_R,Y^*\to Y,Y}\left(Y_{X_I}Y_{X_R}Y_y-\frac{Y^{\mathrm{eq}}_{X_I}Y^{\mathrm{eq}}_{X_R}}{Y^{\mathrm{eq}}_y}Y_y^2\right) \\
& +\langle\sigma v^2\rangle_{Z',Z',X_I\to Z',X_R}\left(Y_{Z'}^2Y_{X_I}-\frac{Y^{\mathrm{eq}}_{Z'}Y^{\mathrm{eq}}_{X_I}}{Y^{\mathrm{eq}}_{X_R}}Y_{Z'}Y_{X_R}\right)+\langle\sigma v^2\rangle_{X_I,X_I,X_I\to Z',X_R}\left(Y_{X_I}^3-\frac{(Y^{\mathrm{eq}}_{X_I})^3}{Y^{\mathrm{eq}}_{Z'}Y^{\mathrm{eq}}_{X_R}}Y_{Z'}Y_{X_R}\right) \\
& -\langle\sigma v^2\rangle_{X_I,X_R,X_R\to Z',X_R}\left(Y_{X_I}Y_{X_R}^2-\frac{Y^{\mathrm{eq}}_{X_I}Y^{\mathrm{eq}}_{X_R}}{Y^{\mathrm{eq}}_{Z'}}Y_{Z'}Y_{X_R}\right)+\langle\sigma v^2\rangle_{Z',X_I,X_R\to X_R,X_R}\left(Y_{Z'}Y_{X_I}Y_{X_R}-\frac{Y^{\mathrm{eq}}_{Z'}Y^{\mathrm{eq}}_{X_I}}{Y^{\mathrm{eq}}_{X_R}}Y_{X_R}^2\right) \\
& +\langle\sigma v^2\rangle_{Z',X_I,Y\to X_R,Y}\left(Y_{Z'}Y_{X_I}Y_y-\frac{Y^{\mathrm{eq}}_{Z'}Y^{\mathrm{eq}}_{X_I}}{Y^{\mathrm{eq}}_{X_R}}Y_{X_R}Y_y\right)-2\langle\sigma v^2\rangle_{X_R,X_R,Y^*\to Y,Y}\left(Y_{X_R}^2Y_y-\frac{(Y^{\mathrm{eq}}_{X_R})^2}{Y^{\mathrm{eq}}_y}Y_y^2\right) \\
& +\langle\sigma v^2\rangle_{Z',Z',Z'\to X_I,X_R}\left(Y_{Z'}^3-\frac{(Y^{\mathrm{eq}}_{Z'})^3}{Y^{\mathrm{eq}}_{X_I}Y^{\mathrm{eq}}_{X_R}}Y_{X_I}Y_{X_R}\right)+\langle\sigma v^2\rangle_{Z',X_I,X_I\to X_I,X_R}\left(Y_{Z'}Y_{X_I}^2-\frac{Y^{\mathrm{eq}}_{Z'}Y^{\mathrm{eq}}_{X_I}}{Y^{\mathrm{eq}}_{X_R}}Y_{X_I}Y_{X_R}\right) \\
& -\langle\sigma v^2\rangle_{Z',X_R,X_R\to X_I,X_R}\left(Y_{Z'}Y_{X_R}^2-\frac{Y^{\mathrm{eq}}_{Z'}Y^{\mathrm{eq}}_{X_R}}{Y^{\mathrm{eq}}_{X_I}}Y_{X_I}Y_{X_R}\right)-\langle\sigma v^2\rangle_{Z',X_R,Y\to X_I,Y}\left(Y_{Z'}Y_{X_R}Y_y-\frac{Y^{\mathrm{eq}}_{Z'}Y^{\mathrm{eq}}_{X_R}}{Y^{\mathrm{eq}}_{X_I}}Y_{X_I}Y_y\right) \\
& +\frac{1}{2}\langle\sigma v^2\rangle_{Z',Y,Y^*\to X_R,X_R}\left(Y_{Z'}Y_y^2-\frac{Y^{\mathrm{eq}}_{Z'}(Y^{\mathrm{eq}}_y)^2}{(Y^{\mathrm{eq}}_{X_R})^2}Y_{X_R}^2\right)-\langle\sigma v^2\rangle_{Z',X_I,X_R\to Y,Y^*}\left(Y_{Z'}Y_{X_I}Y_{X_R}-\frac{Y^{\mathrm{eq}}_{Z'}Y^{\mathrm{eq}}_{X_I}Y^{\mathrm{eq}}_{X_R}}{(Y^{\mathrm{eq}}_y)^2}Y_y^2\right) \\
& -2\langle\sigma v^2\rangle_{Z',X_R,X_R\to Y,Y^*}\left(Y_{Z'}Y_{X_R}^2-\frac{Y^{\mathrm{eq}}_{Z'}(Y^{\mathrm{eq}}_{X_R})^2}{(Y^{\mathrm{eq}}_y)^2}Y_y^2\right)\Bigg].
\end{aligned}
\tag{B.3}
$$

$$
\begin{aligned}
\frac{dY_{Z'}}{dx} = \frac{x}{H}\Bigg[& -\langle\Gamma\rangle_{Z'\to Y,Y^*}\left(Y_{Z'}-\frac{Y^{\rm eq}_{Z'}}{(Y^{\rm eq}_y)^2}Y_y^2\right)-\langle\Gamma\rangle_{Z'\to X_I,X_R}\left(Y_{Z'}-\frac{Y^{\rm eq}_{Z'}}{Y^{\rm eq}_{X_I}Y^{\rm eq}_{X_R}}Y_{X_I}Y_{X_R}\right)\\
& +\langle\Gamma\rangle_{X_R\to Z',X_I}\left(Y_{X_R}-\frac{Y^{\rm eq}_{X_R}}{Y^{\rm eq}_{Z'}Y^{\rm eq}_{X_I}}Y_{Z'}Y_{X_I}\right)\Bigg]\\
& +\frac{s}{Hx^2}\Bigg[-2\langle\sigma v\rangle_{Z',Z'\to X_I,X_I}\left(Y_{Z'}^2-\frac{(Y^{\rm eq}_{Z'})^2}{(Y^{\rm eq}_{X_I})^2}Y_{X_I}^2\right)-2\langle\sigma v\rangle_{Z',Z'\to X_R,X_R}\left(Y_{Z'}^2-\frac{(Y^{\rm eq}_{Z'})^2}{(Y^{\rm eq}_{X_R})^2}Y_{X_R}^2\right)\\
& -2\langle\sigma v\rangle_{Z',Z'\to Y,Y^*}\left(Y_{Z'}^2-\frac{(Y^{\rm eq}_{Z'})^2}{(Y^{\rm eq}_y)^2}Y_y^2\right)+2\langle\sigma v\rangle_{X_R,X_R\to Z',Z'}\left(Y_{X_R}^2-\frac{(Y^{\rm eq}_{X_R})^2}{(Y^{\rm eq}_{Z'})^2}Y_{Z'}^2\right)\\
& -\langle\sigma v\rangle_{Z',Y\to Y^*,Y^*}\left(Y_{Z'}Y_y-\frac{Y^{\rm eq}_{Z'}}{Y^{\rm eq}_y}Y_y^2\right)+2\langle\sigma v\rangle_{X_I,X_I\to Z',Z'}\left(Y_{X_I}^2-\frac{(Y^{\rm eq}_{X_I})^2}{(Y^{\rm eq}_{Z'})^2}Y_{Z'}^2\right)\Bigg]\\
& +\frac{s^2}{Hx^5}\Bigg[\langle\sigma v^2\rangle_{Z',X_I,X_R\to Z',Z'}\left(Y_{Z'}Y_{X_I}Y_{X_R}-\frac{Y^{\rm eq}_{X_I}Y^{\rm eq}_{X_R}}{Y^{\rm eq}_{Z'}}Y_{Z'}^2\right)+\langle\sigma v^2\rangle_{X_I,X_R,Y\to Z',Y}\left(Y_{X_I}Y_{X_R}Y_y-\frac{Y^{\rm eq}_{X_I}Y^{\rm eq}_{X_R}}{Y^{\rm eq}_{Z'}}Y_{Z'}Y_y\right)\\
& +\langle\sigma v^2\rangle_{X_R,X_R,Y\to Z',Y}\left(Y_{X_R}^2Y_y-\frac{(Y^{\rm eq}_{X_R})^2}{Y^{\rm eq}_{Z'}}Y_{Z'}Y_y\right)-\frac{1}{4}\langle\sigma v^2\rangle_{Z',Y,Y^*\to X_I,X_R}\left(Y_{Z'}Y_y^2-\frac{Y^{\rm eq}_{Z'}(Y^{\rm eq}_y)^2}{Y^{\rm eq}_{X_I}Y^{\rm eq}_{X_R}}Y_{X_I}Y_{X_R}\right)\\
& -\langle\sigma v^2\rangle_{Z',Z',X_R\to Z',X_I}\left(Y_{Z'}^2Y_{X_R}-\frac{Y^{\rm eq}_{Z'}Y^{\rm eq}_{X_R}}{Y^{\rm eq}_{X_I}}Y_{Z'}Y_{X_I}\right)+\langle\sigma v^2\rangle_{X_I,X_I,X_R\to Z',X_I}\left(Y_{X_I}^2Y_{X_R}-\frac{Y^{\rm eq}_{X_I}Y^{\rm eq}_{X_R}}{Y^{\rm eq}_{Z'}}Y_{Z'}Y_{X_I}\right)\\
& +\langle\sigma v^2\rangle_{X_R,X_R,X_R\to Z',X_I}\left(Y_{X_R}^3-\frac{(Y^{\rm eq}_{X_R})^3}{Y^{\rm eq}_{Z'}Y^{\rm eq}_{X_I}}Y_{Z'}Y_{X_I}\right)+\frac{1}{4}\langle\sigma v^2\rangle_{X_R,Y,Y^*\to Z',X_I}\left(Y_{X_R}Y_y^2-\frac{Y^{\rm eq}_{X_R}(Y^{\rm eq}_y)^2}{Y^{\rm eq}_{Z'}Y^{\rm eq}_{X_I}}Y_{Z'}Y_{X_I}\right)\\
& -\langle\sigma v^2\rangle_{Z',X_I,X_R\to X_I,X_I}\left(Y_{Z'}Y_{X_I}Y_{X_R}-\frac{Y^{\rm eq}_{Z'}Y^{\rm eq}_{X_R}}{Y^{\rm eq}_{X_I}}Y_{X_I}^2\right)-\langle\sigma v^2\rangle_{Z',Z',X_I\to Z',X_R}\left(Y_{Z'}^2Y_{X_I}-\frac{Y^{\rm eq}_{Z'}Y^{\rm eq}_{X_I}}{Y^{\rm eq}_{X_R}}Y_{Z'}Y_{X_R}\right)\\
& +\langle\sigma v^2\rangle_{X_I,X_I,X_I\to Z',X_R}\left(Y_{X_I}^3-\frac{(Y^{\rm eq}_{X_I})^3}{Y^{\rm eq}_{Z'}Y^{\rm eq}_{X_R}}Y_{Z'}Y_{X_R}\right)+\langle\sigma v^2\rangle_{X_I,X_R,X_R\to Z',X_R}\left(Y_{X_I}Y_{X_R}^2-\frac{Y^{\rm eq}_{X_I}Y^{\rm eq}_{X_R}}{Y^{\rm eq}_{Z'}}Y_{Z'}Y_{X_R}\right)\\
& -\langle\sigma v^2\rangle_{Z',Z',Y\to Z',Y}\left(Y_{Z'}^2Y_y-Y^{\rm eq}_{Z'}Y_{Z'}Y_y\right)-\frac{1}{4}\langle\sigma v^2\rangle_{Z',Y,Y^*\to X_I,X_I}\left(Y_{Z'}Y_y^2-\frac{Y^{\rm eq}_{Z'}(Y^{\rm eq}_y)^2}{(Y^{\rm eq}_{X_I})^2}Y_{X_I}^2\right)\\
& -\langle\sigma v^2\rangle_{Z',X_I,Y\to X_I,Y}\left(Y_{Z'}Y_{X_I}Y_y-Y^{\rm eq}_{Z'}Y_{X_I}Y_y\right)-\langle\sigma v^2\rangle_{Z',X_I,X_R\to X_R,X_R}\left(Y_{Z'}Y_{X_I}Y_{X_R}-\frac{Y^{\rm eq}_{Z'}Y^{\rm eq}_{X_I}}{Y^{\rm eq}_{X_R}}Y_{X_R}^2\right)\\
& -\langle\sigma v^2\rangle_{Z',X_I,Y\to X_R,Y}\left(Y_{Z'}Y_{X_I}Y_y-\frac{Y^{\rm eq}_{Z'}Y^{\rm eq}_{X_I}}{Y^{\rm eq}_{X_R}}Y_{X_R}Y_y\right)-2\langle\sigma v^2\rangle_{Z',Z',Y\to Y^*,Y^*}\left(Y_{Z'}^2Y_y-\frac{(Y^{\rm eq}_{Z'})^2}{Y^{\rm eq}_y}Y_y^2\right)\\
& +\langle\sigma v^2\rangle_{X_I,X_I,Y\to Z',Y}\left(Y_{X_I}^2Y_y-\frac{(Y^{\rm eq}_{X_I})^2}{Y^{\rm eq}_{Z'}}Y_{Z'}Y_y\right)-3\langle\sigma v^2\rangle_{Z',Z',Z'\to X_I,X_R}\left(Y_{Z'}^3-\frac{(Y^{\rm eq}_{Z'})^3}{Y^{\rm eq}_{X_I}Y^{\rm eq}_{X_R}}Y_{X_I}Y_{X_R}\right)\\
& -\langle\sigma v^2\rangle_{Z',X_I,X_I\to X_I,X_R}\left(Y_{Z'}Y_{X_I}^2-\frac{Y^{\rm eq}_{Z'}Y^{\rm eq}_{X_I}}{Y^{\rm eq}_{X_R}}Y_{X_I}Y_{X_R}\right)-\langle\sigma v^2\rangle_{Z',X_R,X_R\to X_I,X_R}\left(Y_{Z'}Y_{X_R}^2-\frac{Y^{\rm eq}_{Z'}Y^{\rm eq}_{X_R}}{Y^{\rm eq}_{X_I}}Y_{X_I}Y_{X_R}\right)\\
& -\langle\sigma v^2\rangle_{Z',X_R,Y\to X_I,Y}\left(Y_{Z'}Y_{X_R}Y_y-\frac{Y^{\rm eq}_{Z'}Y^{\rm eq}_{X_R}}{Y^{\rm eq}_{X_I}}Y_{X_I}Y_y\right)-\frac{1}{4}\langle\sigma v^2\rangle_{Z',Y,Y^*\to X_R,X_R}\left(Y_{Z'}Y_y^2-\frac{Y^{\rm eq}_{Z'}(Y^{\rm eq}_y)^2}{(Y^{\rm eq}_{X_R})^2}Y_{X_R}^2\right)\\
& -\langle\sigma v^2\rangle_{Z',X_R,Y\to X_R,Y}\left(Y_{Z'}Y_{X_R}Y_y-Y^{\rm eq}_{Z'}Y_{X_R}Y_y\right)-\frac{1}{2}\langle\sigma v^2\rangle_{Z',Y,Y\to Y,Y}\left(Y_{Z'}Y_y^2-Y^{\rm eq}_{Z'}Y_y^2\right)\\
& -3\langle\sigma v^2\rangle_{Z',Z',Z'\to Y,Y^*}\left(Y_{Z'}^3-\frac{(Y^{\rm eq}_{Z'})^3}{(Y^{\rm eq}_y)^2}Y_y^2\right)-\frac{1}{4}\langle\sigma v^2\rangle_{Z',Y,Y^*\to Y,Y^*}\left(Y_{Z'}Y_y^2-Y^{\rm eq}_{Z'}Y_y^2\right)\\
& -\langle\sigma v^2\rangle_{Z',X_I,X_R\to Y,Y^*}\left(Y_{Z'}Y_{X_I}Y_{X_R}-\frac{Y^{\rm eq}_{Z'}Y^{\rm eq}_{X_I}Y^{\rm eq}_{X_R}}{(Y^{\rm eq}_y)^2}Y_y^2\right)-\langle\sigma v^2\rangle_{Z',X_R,X_R\to Y,Y^*}\left(Y_{Z'}Y_{X_R}^2-\frac{Y^{\rm eq}_{Z'}(Y^{\rm eq}_{X_R})^2}{(Y^{\rm eq}_y)^2}Y_y^2\right)\\
& -\langle\sigma v^2\rangle_{Z',X_I,X_I\to Y,Y^*}\left(Y_{Z'}Y_{X_I}^2-\frac{Y^{\rm eq}_{Z'}(Y^{\rm eq}_{X_I})^2}{(Y^{\rm eq}_y)^2}Y_y^2\right)\Bigg].
\end{aligned}
\tag{B.4}
$$